

Rheological Properties of Concentrated Polymer Solutions II. A Cone-And-Plate and Parallel-Plate Pressure Distribution Apparatus for Determining Normal Stress Differences in Steady Shear Flow

N. Adams and A. S. Lodge

Phil. Trans. R. Soc. Lond. A 1964 **256**, 149-184
doi: 10.1098/rsta.1964.0002

Email alerting service

Receive free email alerts when new articles cite this article - sign up in the box at the top right-hand corner of the article or click [here](#)

To subscribe to *Phil. Trans. R. Soc. Lond. A* go to: <http://rsta.royalsocietypublishing.org/subscriptions>

RHEOLOGICAL PROPERTIES OF CONCENTRATED POLYMER SOLUTIONS

II. A CONE-AND-PLATE AND PARALLEL-PLATE PRESSURE DISTRIBUTION APPARATUS FOR DETERMINING NORMAL STRESS DIFFERENCES IN STEADY SHEAR FLOW

By N. ADAMS*

Formerly at the British Rayon Research Association, Manchester

AND A. S. LODGE

Department of Mathematics, The Manchester College of Science and Technology, Manchester 1

(Communicated by Sir Geoffrey Taylor, F.R.S.—Received 17 April 1963)

CONTENTS

	PAGE		PAGE
1. INTRODUCTION	150	(a) Preparation and composition of solutions	169
2. THEORY	152	(b) Pressure changes at the start of shear flow	170
3. APPARATUS	155	(c) Pressure distributions with different gaps	172
(a) General description	155	(d) Pressure gradients at various shear rates	174
(b) Dimensions and data	160	(e) The value of $p_{22} - p_{33}$	175
(c) Experimental procedure	160	6. DISCUSSION	179
4. UNWANTED SOURCES OF PRESSURE	160	APPENDIX. THE CONE-AND-PLATE SYSTEM	180
(i) Axis of rotation not perpendicular to stationary plate	161	(a) Conditions at a free liquid boundary	180
(ii) Centrifugal forces	164	(b) Total thrust	182
(iii) Axial movement of rotating member	165	(c) Shear rate	182
(iv) Finite size of holes	167	REFERENCES	184
(v) Perturbations in the state of flow	168		
5. PRESSURE MEASUREMENTS WITH TWO POLYMER SOLUTIONS	169		

For non-Newtonian liquids in steady rectilinear shear flow in which liquid planes $x_2 = \text{constant}$ move parallel to the x_1 -axis of a rectangular Cartesian co-ordinate system $Ox_1x_2x_3$, the three normal components of stress p_{11} , p_{22} , p_{33} , are in general not all equal. Their differences can be determined from the radial distributions of pressure ($-p_{22}$) on the plate of a cone-and-plate system ('cp') or of a pair of parallel plates ('pp') in relative rotation: (a) the quantity $p_{11} + p_{22} - 2p_{33}$ is equal to the pressure gradient $(dp_{22}/d \ln r)_{cp}$; (b) the quantity $p_{22} - p_{33}$ is (under suitable conditions) equal to the value of the pressure $-p_{22}$ at the rim of the rotating member in either system;

* Present address: Authority Health and Safety Branch, United Kingdom Atomic Energy Authority, Harwell, Berks.

and (c) the quantity $p_{22} - p_{33}$ can alternatively be determined from the differences in the values of the pressure gradient $dp_{22}/d \ln r$ obtained (over a range of shear rates) in the two systems. The object of the present paper is to describe a new apparatus for measuring the necessary pressure distributions and in particular to compare the values of $p_{22} - p_{33}$ obtained by the two methods (b), (c).

In the new apparatus (a development of the Roberts–Weissenberg Rheogoniometer), the liquid is sheared in the narrow gap between a rotating member (cone or plate) of diameter 8.8 cm and a stationary flat plate, 20.2 cm \times 12.6 cm. Pressures up to 2×10^3 dyn/cm² are measured to within about 5 dyn/cm² at each of three holes, 0.05 cm in diameter, by means of diaphragm-capacitance gauges which have a response time of a few seconds when used with a test liquid of viscosity 10 P. The apparatus is used with the free liquid boundary either vertical (at the rim of the rotating member) or horizontal (so that the rotating member rotates in a ‘sea’ of liquid filling the lower plate). In the latter case, the radial distribution of pressure can be studied in greater detail by moving the lower plate and its attached pressure gauges horizontally. The alinement of both stationary and rotating members is adjustable. Using a silicone fluid of viscosity 10 P as a Newtonian control liquid in a systematic investigation of the effects of small tilts of the stationary plate about horizontal axes, it is found that a cone-and-plate system is about 12 times more sensitive to tilt than a parallel plate system having the same value of rim gap, and that in neither system can the effect of tilt be completely eliminated by the usual procedure of averaging the pressures recorded with the two senses of rotation.

Measurements on two polymer solutions (polymethylmethacrylate in dimethyl phthalate, polyisobutylene in dekalin) having viscosities in the range 10 to 30 P have been made at shear rates in the range 5 to 100 s⁻¹. Both quantities $p_{11} + p_{22} - 2p_{33}$ and $p_{22} - p_{33}$ are found to be positive ($p_{11} > 0$ for a tensile stress) and to increase steadily with shear rate. Values obtained for $p_{22} - p_{33}$ by methods (b) and (c) are different, being up to seven times greater for method (c). It is not possible, with the solutions used, to assess the accuracy of method (c) owing to uncertainties involved in an extrapolation to zero shear rate. When a constant shear rate is first applied to solutions which have been at rest for 1 or 2 days, records of pressure against time of shearing show two pronounced maxima for the first solution and no maxima for the second solution.

1. INTRODUCTION

Concentrated solutions of very long (high polymer) molecules in solvents of low molecular weight commonly exhibit a variety of unusual and striking rheological properties (e.g. high elastic recovery in shear, high shear-rate-dependent viscosity, thread-forming properties, the tendency to climb up a rotating rod (Weissenberg effect)). These properties cannot be described by the familiar equations of classical hydrodynamics for an incompressible, Newtonian viscous liquid, and the problem of finding the appropriate generalizations of these equations for a given solution or class of solutions is of fundamental importance, for two reasons. First, the effects are large and call for explanation in terms of molecular structure; secondly, the effects arise in many technological processes which involve the flow of polymers in the melt or in concentrated solution. Many forms of rheological equations of state are conceivable and some have been considered in the literature and there is much need for reliable, quantitative experimental data which could be used to narrow the choice between these forms of equations.

In this connexion, the determination of the state of stress in steady shear flow is of particular importance. For an isotropic, incompressible liquid in steady rectilinear shear flow (i.e. in which liquid planes $x_2 = \text{constant}$ move parallel to the x_1 -axis of a rectangular Cartesian co-ordinate system $Ox_1x_2x_3$), there are only three independent stress quantities of rheological interest, namely, a tangential stress component p_{21} and two differences, $p_{11} - p_{22}$ and $p_{22} - p_{33}$ say, of the three normal components of stress p_{11}, p_{22}, p_{33} . In water and low

NORMAL STRESS DIFFERENCES IN STEADY SHEAR FLOW 151

molecular weight solvents generally, the normal stress differences are zero; in concentrated polymer solutions, they are not both zero and give rise to the rod-climbing effects referred to above. Reliable methods of measuring the tangential stress component p_{21} have been known for some time, but the measurement of the normal stress differences is a matter of current research. The object of the present paper is to describe a new apparatus which has been developed to measure these differences; the measurement of $p_{22} - p_{33}$ involves a method which has not hitherto been applied in the literature.

The required values of normal stress differences cannot (in practice) be obtained by direct measurement of stress components in rectilinear shear flow but can be obtained from measurements of certain pressure distributions in suitable curvilinear shear flows (Weissenberg 1947) in which the streamlines are circular. In the Roberts–Weissenberg rheogoniometer (Jobling & Roberts 1959), shear flow between a cone and plate in relative rotation is employed and the radial distribution of pressure on the plate (measured by capillary gauges (Roberts 1957)) yields values for $p_{11} + p_{22} - 2p_{33}$ (from the pressure gradient) and $p_{22} - p_{33}$ (from the pressure at the rim of the cone); the apparatus is also used to measure the total thrust on the cone, from which $p_{11} - p_{22}$ can be determined. The last two methods, for determining $p_{22} - p_{33}$ and $p_{11} - p_{22}$, are only valid provided the required state of shear flow persists right up to the free boundary at the rim of the cone; in the Appendix, it is shown that this can be the case only if the free boundary has a particular shape which is unlikely to be accurately realized in practice; the methods are therefore liable to error, of an amount as yet unassessed. The same criticism must be brought against another method (Pollett 1955) in which thrusts are measured on a lower plate and an annular guard ring.

It is therefore important to seek an alternative method of determining $p_{22} - p_{33}$ from measurements which do not depend on the shape of the free liquid boundary. The pressure gradient in the cone-and-plate system gives one combination ($p_{11} + p_{22} - 2p_{33}$) of the required stress differences. For the shear flow between parallel plates in relative rotation, the curvature pattern of the flow surfaces is different, and accordingly the corresponding pressure gradient gives a different combination ($p_{11} - p_{33} + Gd(p_{22} - p_{33})/dG$, where G denotes shear rate) of normal stress differences. On the reasonable assumption that the change of curvature pattern does not affect the values of normal stress differences at a given shear rate, these two measurements of pressure gradient can be combined to give a pair of simultaneous equations sufficient to determine both the required normal stress differences, and $p_{22} - p_{33}$ in particular. The theory of this method is outlined in §2. It is not open to the criticism levelled above at the other methods, but it does have difficulties of its own, arising from the need to make a certain extrapolation to zero shear rate.

Since this method involves measurement of pressure distributions rather than total thrust, a new apparatus has been built similar in principle to the Roberts–Weissenberg rheogoniometer but having quick-response diaphragm-capacitance pressure gauges (cf. Ward & Lord 1957) instead of slow-response capillary gauges (Garner, Nissan & Wood 1950). The apparatus, which is described in §3, differs in other details: both rotating and stationary members are adjustable in alinement, and the stationary member can be moved in a direction at right angles to the axis of rotation to enable the pressure distribution to be studied in any required detail when the rotating member rotates in a ‘sea’ of liquid. (It is permissible to use a ‘sea’ of liquid with the present method since conditions at and outside

the rim of the rotating member do not affect the values of pressure *gradient* at points inside the rim of the rotating member.)

It is known that apparatus of the type used here, which involves the flow of a viscous liquid in a narrow gap between rigid members of large area, is peculiarly liable to the generation of large, spurious pressures from small tilts of the members, from small end-movements in the bearing of the rotating member, and from the presence of holes of finite size used in the measurement of pressure. These and other systematic errors are carefully considered (§4), and in particular a systematic investigation of the effects of tilt with a viscous Newtonian liquid is made for both cone-and-plate and parallel plate systems; this is believed to be the first time such data have been published for the cone-and-plate system.

In order to try out the apparatus, pressure distributions have been measured with two polymer solutions (§5). The performance of the apparatus is considered to be satisfactory because (i) in the cone-and-plate system the pressure distribution is found to have the expected form over most of the plate and to be independent of gap angle when measured at constant shear rate; and (ii) in the parallel plate system, the pressure gradient at constant shear rate is found to be independent of gap size. For both solutions, the pressure gradients in the two systems yield positive values for $p_{22} - p_{33}$ which increase steadily with increase of shear rate. The rim pressures also yield positive, steadily increasing values for $p_{22} - p_{33}$ but the latter values are significantly smaller than the former values; the two methods thus lead to discordant results.

The response time (a few seconds) of the pressure measuring system is short enough for transient changes in pressure to be followed when a constant shear rate is first applied to a fresh solution. The two solutions used are found to exhibit very different transient behaviour.

A brief reference to some of the present results has been published already (Lodge 1960*a*, 1961*a*; Adams 1960).

2. THEORY

The theory underlying the present method of determining normal stress differences from pressure gradients in cone-and-plate and parallel plate systems may be derived from the following assumptions.

(i) The liquid can be treated as an incompressible deforming continuum in which a symmetric stress tensor is everywhere defined.

(ii) The state of flow between cone and plate in relative rotation is such that each infinitesimally thin cone of liquid (referred to below as a 'shearing surface'), having the same apex and axis as the rigid cone, rotates rigidly about this axis with a constant angular velocity whose value depends on the semi-vertical angle of the liquid cone.

(iii) The state of flow between parallel plates in relative rotation is such that each infinitesimally thin plane of liquid (referred to below as a 'shearing surface'), parallel to the plates, rotates rigidly about the common axis of rotation with a constant angular velocity whose value depends on the distance from the fixed plate.

(iv) In both states of flow, the physical components p_{ij} ($i, j = 1, 2, 3$) of the stress tensor satisfy the relations,

$$p_{31} = p_{13} = p_{32} = p_{23} = 0, \quad (2.1)$$

NORMAL STRESS DIFFERENCES IN STEADY SHEAR FLOW 153

when the 1-direction is taken parallel to the streamlines and the 2-direction is taken normal to the shearing surfaces. (p_{ij} are equal to the Cartesian components of the stress tensor in a local rectangular Cartesian co-ordinate system $Ox_1x_2x_3$ with origin O in the liquid element considered and axes Ox_1 and Ox_2 parallel to the streamlines and normal to the shearing surfaces.)

(v) The differences $p_{11} - p_{22}$, $p_{22} - p_{33}$ of normal stress components at any point in the liquid in either state of flow depend only on the value G of the shear rate (defined below) at that point.

(vi) The differences $p_{11} - p_{22}$, $p_{22} - p_{33}$ may be expressed as even functions of the variable G which tend to zero at least as fast as G^2 as G tends to zero.

(vii) The effects of inertia are negligible.

The shear rate (or velocity gradient) G may be defined as follows. For a liquid in any state of flow with covariant components of velocity v_i relative to a general system of co-ordinates y_1, y_2, y_3 , the rates of change of separation of particles in a given volume element are completely described by the values of the components $\frac{1}{2}(v_{i,j} + v_{j,i})$ of the symmetric part of the covariant derivative of the velocity field. For the flow between cone and plate, we take y_1, y_2, y_3 equal to the coordinates r, θ, ϕ of a spherical polar coordinate system with origin at the cone apex and axis $\theta = 0$ along the axis of rotation. For the flow between parallel plates, we take y_1, y_2, y_3 equal to the co-ordinates r, ϕ, z of a cylindrical polar co-ordinate system with axis $r = 0$ along the axis of rotation. It can then be shown that the physical components

$$\frac{1}{2}(g_{ii}g_{jj})^{-\frac{1}{2}}(v_{i,j} + v_{j,i}) = e_{ij} \quad (i, j \text{ not summed}) \quad (2.2)$$

(where g_{ij} denote the components of the metric tensor) of the rate-of-strain tensor have the same form for both states of flow, namely, all e_{ij} are zero except for

$$e_{12} = e_{21} = \frac{1}{2}G \quad (\text{say}). \quad (2.3)$$

When account is taken of the stress equations of motion, it can also be shown that the values of shear rate in units of second⁻¹ are given by the equations

$$G = \Omega r/z_0 \quad (\text{parallel plates}), \quad (2.4)$$

and

$$G = \Omega/\Delta\theta \quad (\text{cone-and-plate}), \quad (2.5)$$

where Ω is the angular velocity of the rotating member (in radians per second), z_0 is the separation of the parallel plates and $\Delta\theta$ the angle in radians of the gap between cone and plate; the approximation in (2.5) is shown in the Appendix to be very good for gap angles not greater than a few degrees. It should be noted that, with this definition, the shear rate G changes sign when the direction of rotation is reversed.

For the points on the plate of the cone-and-plate system (with the plate horizontal), one of the stress equations of motion takes the form

$$r dp_{33}/dr = p_{11} + p_{22} - 2p_{33}, \quad (2.6)$$

when account is taken of (iv) and (vii). From (v) and (2.5), it follows that $p_{22} - p_{33}$ is independent of r ; hence $dp_{33}/dr = dp_{22}/dr$, and (2.6) becomes

$$(r dp_{22}/dr)_{cp} = p_{11} + p_{22} - 2p_{33}. \quad (2.7)$$

The suffixes cp , pp are used to distinguish between values appropriate to the cone-and-plate system and the parallel plate system. The quantity on the left-hand side of this equation is measurable, since $-p_{22}$ is equal to the pressure on the plate. The usual sign convention is used, in which $p_{22} > 0$ for a tensile stress. Since the right-hand side of (2.7) is a combination of $p_{11} - p_{22}$ and $p_{22} - p_{33}$ which (by (v) and (2.5)) are independent of r , it follows from (2.7) that p_{22} varies linearly with $\log r$.

For points on the plate of the parallel plate system (with the plates horizontal), one of the stress equations of motion takes the form

$$r dp_{33}/dr = p_{11} - p_{33} \quad (2.8)$$

when account is taken of (2.1) and (vii). From (v) and (2.4) it follows that

$$r d(p_{22} - p_{33})/dr = G d(p_{22} - p_{33})/dG,$$

and hence (2.8) implies that

$$\left(r \frac{dp_{22}}{dr} \right)_{pp} = p_{11} - p_{33} + G \frac{d}{dG} (p_{22} - p_{33}). \quad (2.9)$$

Again, the left-hand side of this equation is a measurable quantity, since $-p_{22}$ is equal to the pressure on the plate.

Now it follows from (v) that equations (2.7) and (2.9) may be regarded as simultaneous equations in two dependent variables, $p_{11} - p_{22}$ and $p_{22} - p_{33}$, and one independent variable, G , the left-hand sides being regarded as given functions of G . By subtraction, we obtain the equation

$$\left(G \frac{d}{dG} - 1 \right) (p_{22} - p_{33}) = \left(r \frac{dp_{22}}{dr} \right)_{pp} - \left(r \frac{dp_{22}}{dr} \right)_{cp}. \quad (2.10)$$

Integrating this equation, we finally obtain the result

$$(p_{22} - p_{33})_G = G \int_0^G \left\{ \left(r \frac{dp_{22}}{dr} \right)_{pp} - \left(r \frac{dp_{22}}{dr} \right)_{cp} \right\}_{G'} \frac{dG'}{G'^2}. \quad (2.11)$$

The constant of integration has been determined by using the fact that

$$p_{22} - p_{33}, \quad (r dp_{22}/dr)_{pp}, \quad \text{and} \quad (r dp_{22}/dr)_{cp}$$

are unchanged in value when the sign of G is changed; this follows from (vi), (2.7) and (2.9).

Equations (2.7) and (2.11) are the basic equations of the present paper. They show that the values of $p_{22} - p_{33}$ and $p_{11} - p_{22}$ at any given value of G may be obtained from measurements of pressure gradient at points away from the rim of the rotating member in the cone-and-plate and parallel plate systems, the measurements being taken over a range of values of shear rate from zero to G .

In practice, measurements cannot be made at zero shear rate and an extrapolation to zero shear rate will have to be made in evaluating the integral in (2.11). If (as we assume) (vi) is true, then it follows from (2.10) that the quantity in curly brackets in the integrand of (2.11) tends to zero at least as fast as G^2 as G tends to zero; hence the integral converges at the lower limit of integration and, moreover, if measurements can be made at values of G low enough for this region of 'G²-dependence' to be reached, the integrand will be constant (or tend to zero with G if the dependence is G^4 or higher) in this region and the extrapolation to zero shear rate can be made with confidence. Such a region was not reached with

the two solutions used in the measurements reported here and accordingly some uncertainty attaches to the extrapolations made. Markovitz (1957) has pointed out that the method considered here would be of low sensitivity in any region in which the normal stress differences are proportional to $|G|^\alpha$ with $\alpha \approx 1$. In such a region, equation (2.10) takes the form

$$(\alpha - 1)(p_{22} - p_{33}) = (r \, dp_{22}/dr)_{pp} - (r \, dp_{22}/dr)_{cp}; \quad (2.12)$$

since $\alpha - 1$ is small, the right-hand side must be small, and thus $p_{22} - p_{33}$, being determined by the ratio of two small quantities, is liable to substantial error. This difficulty will not arise for liquids for which accurate measurements can be made at values of G small enough for α to take the value 2 or more.

Probably the most important of the assumptions underlying the method is (v). It would not be valid (and the present method would not apply) if the normal stress differences depended on curvature of the streamlines or on spatial gradients of the strain history; while such a possibility cannot be ruled out, it does seem physically unlikely for homogeneous materials and leads to such an increase in the complexity of the possible forms of rheological equation of state that we are justified in setting aside this possibility until experimental evidence forces us to consider it. Accordingly, we confine our attention to the still very large class of rheological equations of state for homogeneous incompressible isotropic materials which are such that the stress tensor in any given volume element is determined, to within an additive isotropic stress, by the strain history of that element alone; it can then be shown that assumptions (iv), (v) and (vi) are valid (Coleman & Noll 1959). It may be noted that an explicit dependence of stress on spatial gradients of strain history could lead to a dependence of $p_{11} + p_{22} - 2p_{33}$ on curvature of the streamlines and of the surfaces $r = \text{constant}$; in this case, the pressure on the plate in the cone-and-plate system might not vary linearly with $\ln r$.

Of the remaining assumptions, (i) is fundamental to the subject, while (ii), (iii) and (vii) relate to the states of flow set up in the apparatus. (vii) is shown to be valid from an estimate of the effects of inertia on the pressure distribution made from the control measurements with a silicone fluid (§4). Direct consequences of (ii), (iii) are checked by changing the gap between parallel plates and the angle of the gap between cone and plate. Moreover, the state of flow (iii) between parallel plates has been shown to represent an exact solution of the stress equations of motion and boundary conditions when inertia is neglected. The state of flow (ii) between cone and plate, on the other hand, does not in general represent an exact solution of the stress equations of motion even when inertia is neglected (Oldroyd 1958); however, further calculations (at present in course of publication) suggest that (ii) should represent an approximate solution valid for the small values of the gap angle used here (§4).

3. APPARATUS

(a) *General description*

The main features of the apparatus are shown in vertical projection in figure 1. Unless the contrary is stated, all capital letters labelling parts of the apparatus refer to figure 1. The liquid under investigation is contained in a shallow, horizontal trough S and is sheared in the gap between a stationary plate R (which forms the base of the trough S) and a rotating cone (or plate) T . The cone T rotates in the headstock H of a 70 mm Pultra centre lathe

(not shown in the figure) with headstock built up to 90 mm. This lathe is rigidly mounted with its axis vertical and its headstock uppermost. The cone T is rigidly attached by three pairs of adjusting screws (one pair J , being shown) to a plate V attached to a Collet-type member W which is held in position on the shaft I by screwing down the drawbar D (which passes through the centre of the hollow shaft I). The shaft I is rotated in cylindrical journal bearings G , Y by means of a 'Velodyne' continuously variable speed servomotor operating through a 50:1 reduction worm gear box and a vertical universal coupling attached to the top of the draw bar D (motor and gear box are not shown).

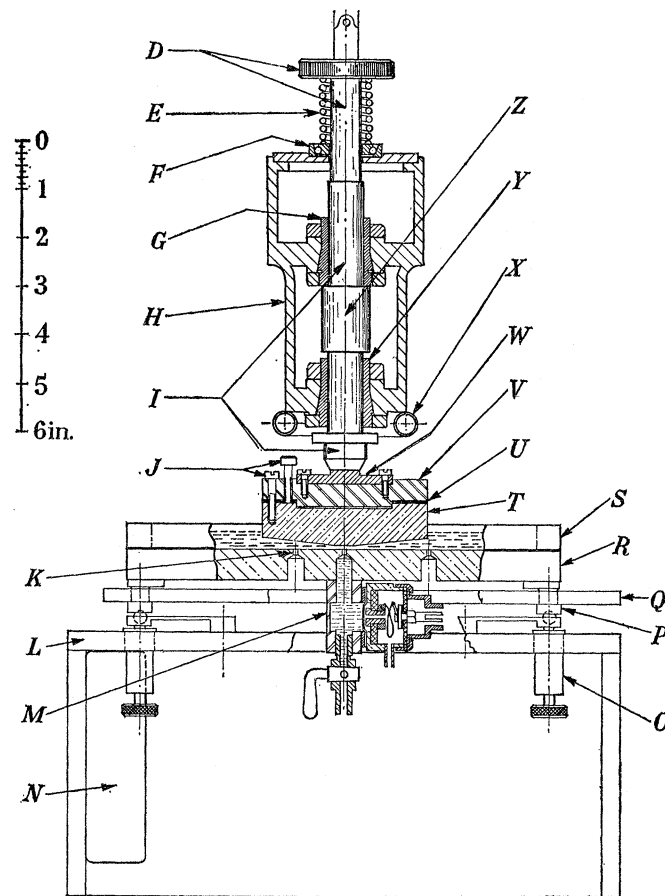


FIGURE 1. Pressure distribution apparatus showing vertical section through cone T , plate R , and pressure gauge M (rotated for clarity from its actual position). The frame L and the headstock H are attached to a vertical lathe bed (not shown). The drawbar D is driven by a motor and reduction gear (not shown). Two pressure gauges have been omitted.

The vertical position of the rotating shaft I is determined by the sleeve Z (rigidly attached to I) whose top face is held in contact with (and rotates against) the lower end of the journal bearing G ; this contact is maintained by means of the spring E which is held in compression between the drawbar D and a thrust ball race F . The apparatus at first gave rise to an appreciable periodically varying pressure in the test liquid due to a small vertical movement of amplitude about $300 \mu\text{in.}$ in the rotating member; by lapping the upper face of the sleeve Z on a suitable mandrel, the vertical movement was reduced by a factor of 10 and the periodic variation of pressure was substantially eliminated. The journal

NORMAL STRESS DIFFERENCES IN STEADY SHEAR FLOW 157

bearings *G*, *Y* were lubricated from time to time with a light machine oil. During a period of about 2 years' use, a small reduction in amplitude of the vertical movement was observed.

The plate *R* is attached to a light, rigid duralumin frame *L* by means of a kinematic mounting consisting of 3 balls (*D*, *G*, *I* in figure 2) in horizontal *V*-grooves, concurrent (near *C*, figure 2) when produced. The plate *R* is held in contact with the frame *L* by means of a thin duralumin plate *Q* which, resting on feet *P*, is pulled down on to the frame *L* by means of a centrally placed spring-loaded screw (not shown). The vertical position of two (*D*, *I*, figure 2) of the three balls is adjustable by means of differential screws *O*; these enable the plate *R* to be tilted through small angles about horizontal axes of any desired orientation. The whole of the lower plate assembly *R*, *S*, etc., can be moved horizontally and vertically by means of the lathe cross feeds (not shown) to which the frame *L* is fixed.

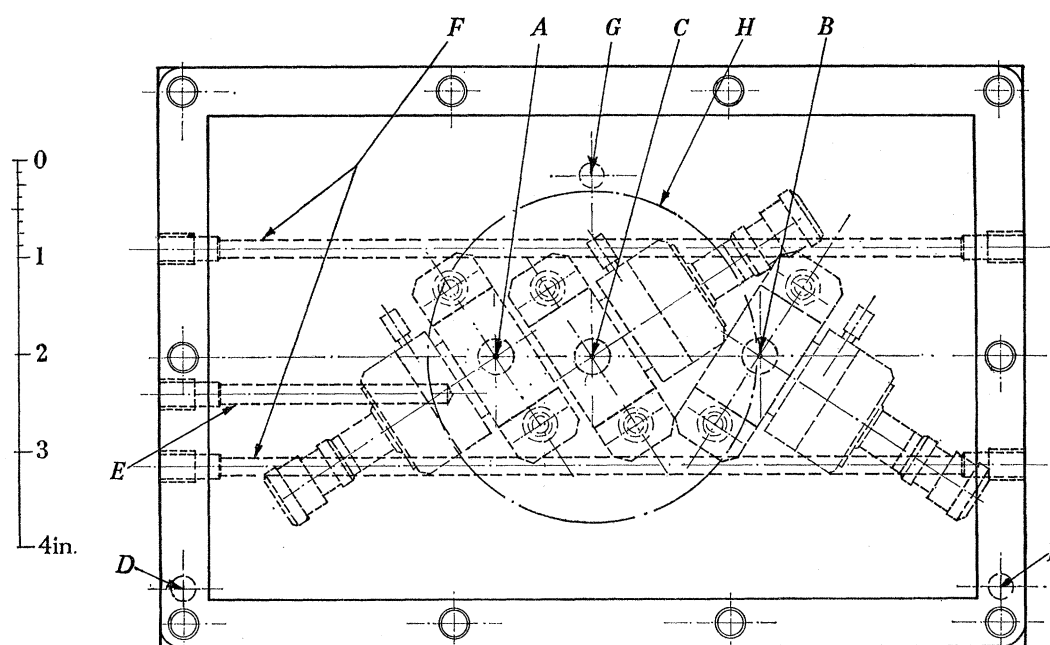


FIGURE 2. View of stationary plate from above, showing the position of holes *A*, *C*, *B*, rim *H* of rotating member and arrangement of pressure gauges (broken lines) attached to underside of plate. Holes *F*, *E* are for water circulation and thermometer.

Pressures at three holes *K* (*A*, *C*, *B* figure 2) are measured by diaphragm-capacitance gauges *M* bolted to the underside of the plate *R*. The ground face of *R* and the lapped faces of the gauges give liquid-tight joints. The disposition of the gauges is shown in the plan view of the plate *R* given in figure 2; for clarity, only one gauge *M* is shown in figure 1 and that in a slightly false view, being rotated about a vertical axis through the hole in the plate. The diaphragm-capacitance gauge, developed for use with this apparatus, is described in detail elsewhere (Lodge 1960*b*). A change of pressure near the hole in the plate *R* is transmitted through the test liquid in the gauge to a diaphragm whose movement gives rise to a change of capacity to a fixed electrode; this is amplified and converted to a change of current by a very stable high-gain battery-operated circuit, of the type due to Attree (1952), mounted in a screened box *N* on the frame *L*, there being one such circuit for each gauge. For the measurement of steady pressures, the gauges are used as null indicators; the outputs from the Attree circuits are connected in turn to a microammeter (0 to 50 μ A range),

and adjustable air pressures are applied to the electrode sides of the diaphragms and measured by means of a calibrated inclined-tube manometer of range 0 to 1.5 in. water gauge. For the measurement of a varying pressure at a single hole, the output from one gauge is amplified by a Fielden type PM2 proximity meter which is used to operate a Record millimeter pen recorder.

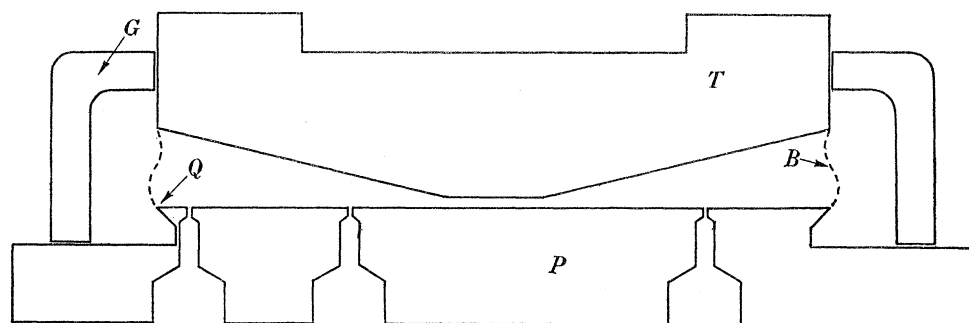


FIGURE 3. Arrangement for confining the liquid to the gap between cone T and plate P . (Vertical section through axis of rotation and line of pressure-measuring holes.) The sharp edge Q on the auxiliary plate P enables the liquid when filling the gap between P and T to maintain a free boundary B . The guard ring G reduces solvent evaporation.

The temperature of the plate R , measured by a thermometer placed in the hole E (figure 2), is kept constant to within 0.1°C by means of water from a thermostat tank pumped through holes F (figure 2) in the plate and through a coil X making good thermal contact with the bearing housing. The cone T is insulated from the mounting V by a cork shim U . Ambient room temperature is controlled to within about $\pm 0.5^\circ\text{C}$ of the plate temperature. Solvent evaporation is reduced by means of a glass plate (not shown) resting on top of the trough S and having a clearance hole for the rotating member T ; a circular annulus of thin polyethylene sheet fits on the side of the rotating member T and rotates against the top of the glass plate to reduce evaporation from the gap between the clearance hole in the glass plate and the rotating member.

When the liquid is to be confined to the gap between rotating and stationary members, the auxiliary plate P shown in figure 3 is clamped on top of the plate R of figure 1 with the sharp rim Q underneath the rim of the rotating member T and the holes suitably disposed above the corresponding holes in the plate R of figure 1. Solvent evaporation is reduced in this case by means of a duralumin guard ring G resting on the plate P and making a sliding fit on the side of the rotating member T . It was found that the use of a smaller set of holes in P (not shown in figure 3) led to too great an instability in the zero readings of the pressure-measuring system; this was believed to arise from expansion and contraction of the liquid in the gauges (due to small temperature fluctuations) causing larger pressure fluctuations due to the increased resistance to flow with the smaller holes. The dynamic temperature coefficients of the gauges filled with liquid are rather large.

(b) *Dimensions and data*

(i) *Stationary plate.* The plate R is made from a stainless steel (B.S. En 58J, 18/8 molybdenum) chosen for its dimensional stability, suitably heat-treated and surface-ground so that the upper surface is planar to within $200\ \mu\text{in.}$ in the temperature range 20 to 35°C .

NORMAL STRESS DIFFERENCES IN STEADY SHEAR FLOW 159

The working surface measures 20.2 cm by 12.6 cm. The holes A , C , B (figure 2) are each of diameter 0.05 cm; their centres are collinear and have separations $AC = 2.54$ cm, $CB = 4.45$ cm.

(ii) *Auxiliary plate.* The auxiliary plate P (figure 3), made from the same steel, has a circular working surface of diameter 8.82 cm surface-ground so as to be planar to within $50 \mu\text{in}$. The holes are of diameter 0.07 cm and are at distances 1.90 cm, 2.82 cm and 4.02 cm from the centre of the plate. The plate has also a set of holes (not used in the present measurements) of diameter 0.05 cm at similar distances from the centre of the plate and lying on a line at right angles to the line of centres of the first set.

(iii) *Horizontal traverse.* In the systematic measurements of pressure gradients at different shear rates, three particular positions α , β , γ of the horizontal traverse are used. The corresponding distances of the three holes from the axis of rotation are given in table 1; holes A , C are always on one side of the axis of rotation, hole B on the other. Position β is chosen to make A and B equidistant from the axis; positions α , γ are chosen so that the distance of A from the axis in either position equals the distance of B from the axis in the other position.

TABLE 1. DISTANCES OF HOLES FROM AXIS OF ROTATION

traverse position	distance (cm) of hole centre from axis		
	A	B	C
α	4.13	2.86	1.59
β	3.49	3.50	0.95
γ	2.86	4.13	0.32

The stationary plate R is alined to within 0.0002° of the perpendicular to the axis of rotation, usually in the intermediate traverse position β . Owing to imperfections in the cross-feed slide, the horizontal movement of the plate from position α to position γ (a movement of 1.27 cm) introduces a more-or-less systematic tilt of about 0.01° and a vertical movement (of the plate as a whole) of not more than $50 \mu\text{in}$.

(iv) *Rotating members.* The rotating members R are made from mild steel with the working surfaces ground. Each is of diameter 8.80 cm. The surface of the flat plate is planar to within $100 \mu\text{in}$. Two cones are used, giving gap angles of about 3° and 5° ; for the 3° cone, the semi-vertical angle is $90^\circ - (3.231 \pm 0.004)^\circ$ and the apex is ground off flat to a depth of 0.0037 in. the corresponding figures for the 5° cone are $90^\circ - 5.167^\circ$ and 0.0059 in. The gap between rotating and stationary members is set to an accuracy of 0.0005 in.

As the speed of rotation is increased from 47 to 5 s per revolution, the amplitude of the vertical movement of the rotating member decreases from 28 to $15 \mu\text{in}$. for one sense of rotation and from 54 to $15 \mu\text{in}$. for the other

The following instruments were used in obtaining the above data. Plate flatness: a Johanssen straight edge, with slip gauges; cone angles: a sine bar with verification (for the 3° cone) from surface co-ordinate readings taken with a Universal Measuring Machine (MU 214B); vertical movement of rotating member: a Fielden Proximity Meter with a capacity probe placed under the centre of the rotating flat plate.

(v) *Pressure measurement.* The overall zero stability of each pressure-measuring unit when used with the plate R and test liquids of viscosity up to 30 P is usually about 4 dyn/cm^2 over a period of a few hours. Pressures are measured in the range 10 to 3000 dyn/cm^2 .

With the use of a vertical U-tube manometer as standard, a spot check on the accuracy of the pressure-measuring system gave percentage errors of -0.5 , 0.0 , and -1.5 for measurements of pressure at holes A , B , and C . (Hole C is not used in most of the measurements reported below.) Approximate values of sensitivity of the gauges at A , B and C are 2, 2 and $1.6 \text{ pF}/10^3 \text{ dyn/cm}^2$. For each gauge with its Attree circuit, the overall magnification (i.e. the ratio of movement of the output microammeter pointer to the estimated central deflexion of the diaphragm) is about 2×10^5 . The dynamic temperature coefficient of each gauge, when filled with a 30 P liquid, is about $10^3 \text{ dyn cm}^{-2} \text{ degC}^{-1} \text{ min}^{-1}$.

(c) *Experimental procedure*

The pressure gauges are first filled slowly from below with the liquid under investigation until this appears above the holes K and the taps are then closed. The lower surface of the rotating member T is alined by adjusting the pairs of screws J until, on rotating the member T , the change of capacity measured by a small stationary flat probe placed under the rim of T is sufficiently small. The alinement of the stationary plate R is then adjusted by means of the differential screws O until, on rotating the member T , the change of capacity between a probe attached to (and rotating with) T and the upper face of R is sufficiently small. The capacity probe is then removed, sufficient liquid added to the trough S , R and the lower plate assembly is moved upwards until the required gap between stationary and rotating members is obtained. With the present arrangement of the drive, a change from one type of rotating member to another necessitates removal of the headstock H ; when this is replaced the alinement of both rotating and stationary members is checked and adjusted when necessary.

The horizontal traverse being adjusted to the required position, the member T is rotated at a constant speed (measured by visual timing) and the pressures measured when steady; the sense of rotation is then reversed, the speed checked and the steady values of pressure again measured. The horizontal traverse is then altered and the procedure repeated.

4. UNWANTED SOURCES OF PRESSURE

The pressure distributions which it is desired to measure in the present apparatus arise from inequality between the normal stress components at each point in the liquid. In practice, however, the following unwanted sources of pressure must be considered:

- (i) Axis of rotation not perpendicular to stationary plate.
- (ii) Centrifugal forces.
- (iii) Axial movement of rotating member.
- (iv) Finite size of holes used for pressure measurement.
- (v) Perturbations to state of flow in cone-and-plate system.

Of these sources, it is known that (i) and (iii) can give rise to large pressures. For liquids of given density and viscosity, it is likely that sources (i), (ii), (iii) and (iv) give rise to pressures whose order of magnitude does not depend on the differences of normal stress components in shear flow; accordingly, the importance of these sources is assessed, by calculation and by experiment, using liquids with supposedly equal normal stress components (referred to below as Newtonian liquids) and with density and viscosity comparable to those of the liquids with unequal normal stress components used in subsequent experiments.

Source (v) arises only when the normal stress components are unequal and is dealt with by an approximate calculation. The conclusion is that the present apparatus can be used in such a manner that the above sources of pressure are either negligible or are small and can be corrected for satisfactorily. This conclusion is confirmed to some extent by the self-consistency of the data obtained with liquids having unequal normal stress components when different gap angles or gap sizes are used (figures 10 and 11).

(i) *Axis of rotation not perpendicular to stationary plate*

If the surface of the rotating flat plate is perpendicular to the axis of rotation but the stationary plate is not, the resulting non-parallelism of the two plates results in a converging flow in one half of the gap and a diverging flow in the other half, the two halves being separated by the vertical plane through the line of greatest slope of the non-horizontal plate, the other plate being supposed horizontal. When the gap is narrow and the liquid is viscous, a very small degree of non-parallelism can give rise to a large pressure maximum in the region of converging flow and an equally large pressure minimum in the region of diverging flow. This so-called 'wedge effect' or 'Michell bearing effect' has been investigated for a system of two flat plates in relative rotation experimentally by Greensmith & Rivlin (1953) and theoretically by Taylor & Saffman (1957) who show that, for a Newtonian incompressible liquid, the pressure distributions over the two halves of either plate are symmetrical apart from the difference of sign, and that the two distributions change places when the direction of rotation is reversed. According to these calculations, therefore, the wedge effect is eliminated if the average is taken of the pressures recorded with the two senses of rotation. No comparable experimental or theoretical investigation appears to have been published for the wedge effect between cone and plate.

In the present apparatus, the stationary plate can readily be tilted by a continuously variable amount about horizontal axes making any desired angles with the line of pressure-measuring holes; this enables the wedge effect to be investigated in rather greater detail than has hitherto been possible. The results of such an investigation are shown in figure 4 for the parallel plate system and in figure 5 for the cone-and-plate system. The liquid used in this investigation is a silicone fluid (MS 200/1000 cS; viscosity 10.6 P (cf. figure 8)) believed to have substantially equal normal stress components; this belief is consistent with the pressure distributions actually obtained. In order to employ the horizontal traverse of the stationary plate so as to measure the pressure distribution in sufficient detail, the apparatus is here used with the rotating member rotating in a 'sea' of liquid.

For the plate-and-plate system, it is seen that the pressure distribution measured at points along a line which passes through the axis of rotation and is *perpendicular* to the line of greatest slope (figure 4(b)) displays the symmetrically disposed maximum and minimum which interchange on reversal of the direction of rotation in at least qualitative agreement with the predictions of Taylor & Saffman; moreover, the average of pressures recorded for the two directions of rotation is almost zero, the slightly negative values of this average being attributable to the effects of centrifugal forces (cf. §4(ii), below). On the other hand, the distribution of pressure along the line of greatest slope (figure 4(c)) displays a small but quite definite non-uniformity which is independent of the direction of rotation; this conflicts with the calculations of Taylor & Saffman who predict zero pressure at all points on the

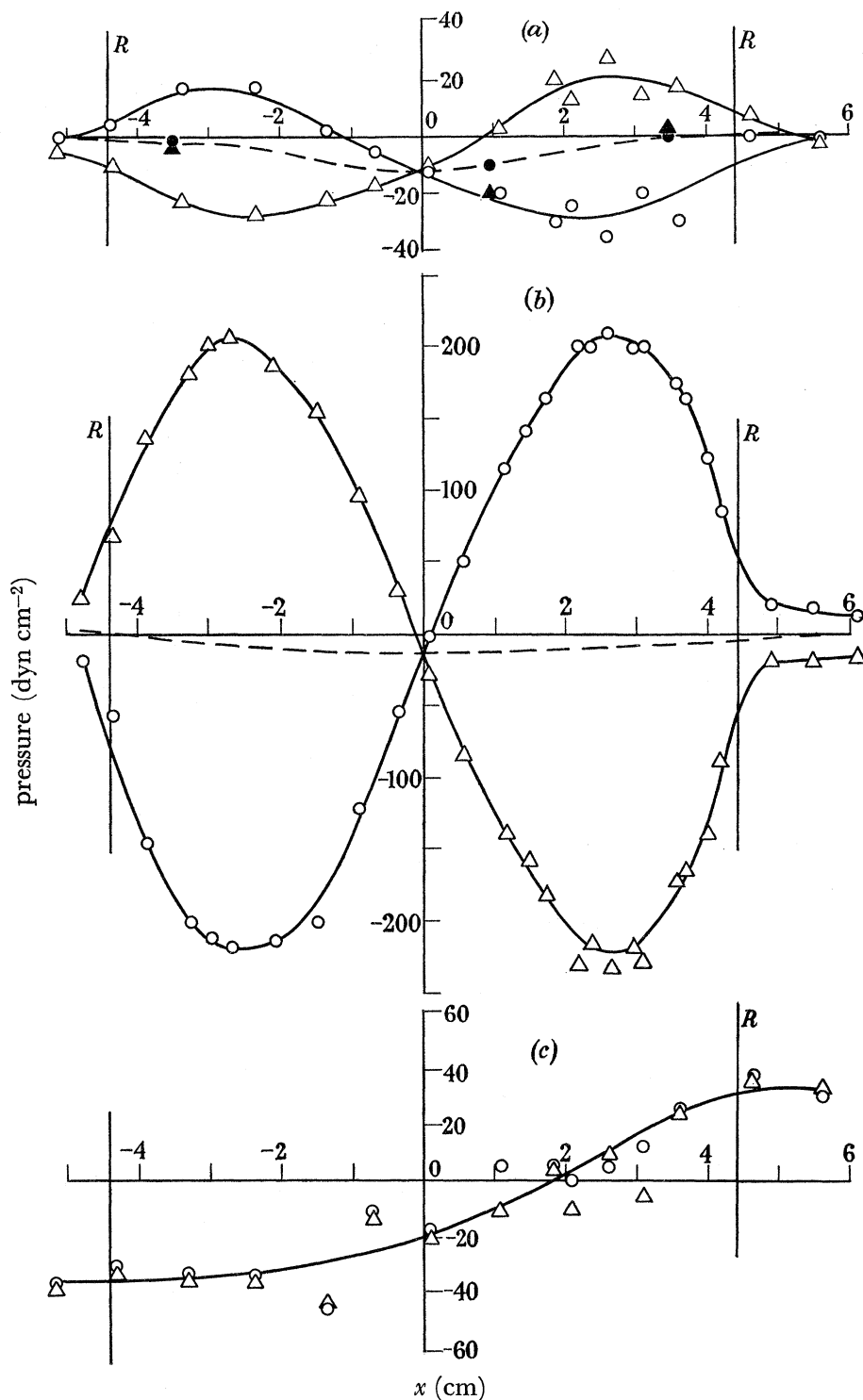


FIGURE 4. Pressure distributions when the axis of rotation is not perpendicular to the stationary plate: plate-and-plate system. (a) Axis nominally perpendicular: initial alinement $\epsilon < 0.0007^\circ$ ($\bullet\blacktriangle$); on return to same setting of differential screws after data of (b), (c) are taken ($\circ\triangle$). (b) $\epsilon = 0.23^\circ$; distribution of pressure along a line at right angles to a line of greatest slope. (c) $\epsilon = 0.37^\circ$; distribution of pressure along a line of greatest slope. Gap larger on positive x -axis. $\epsilon =$ angle between axis of rotation and perpendicular to stationary plate. Speed of rotation 0.3 rev/s; circles and triangles represent two senses of rotation. Separation of plates at axis of rotation, 0.100 in. Silicone fluid, 10.6 P. The co-ordinate axis Ox coincides with the line of pressure-measuring holes, O being on the axis of rotation. $R \equiv$ rim of rotating plate.

NORMAL STRESS DIFFERENCES IN STEADY SHEAR FLOW 163

line of greatest slope. However, since the observed pressure distribution is approximately symmetrical, apart from a change of sign, about the axis of rotation, errors arising from this source can be reduced by taking the average of pressures recorded at points on opposite sides of and equidistant from the axis of rotation.

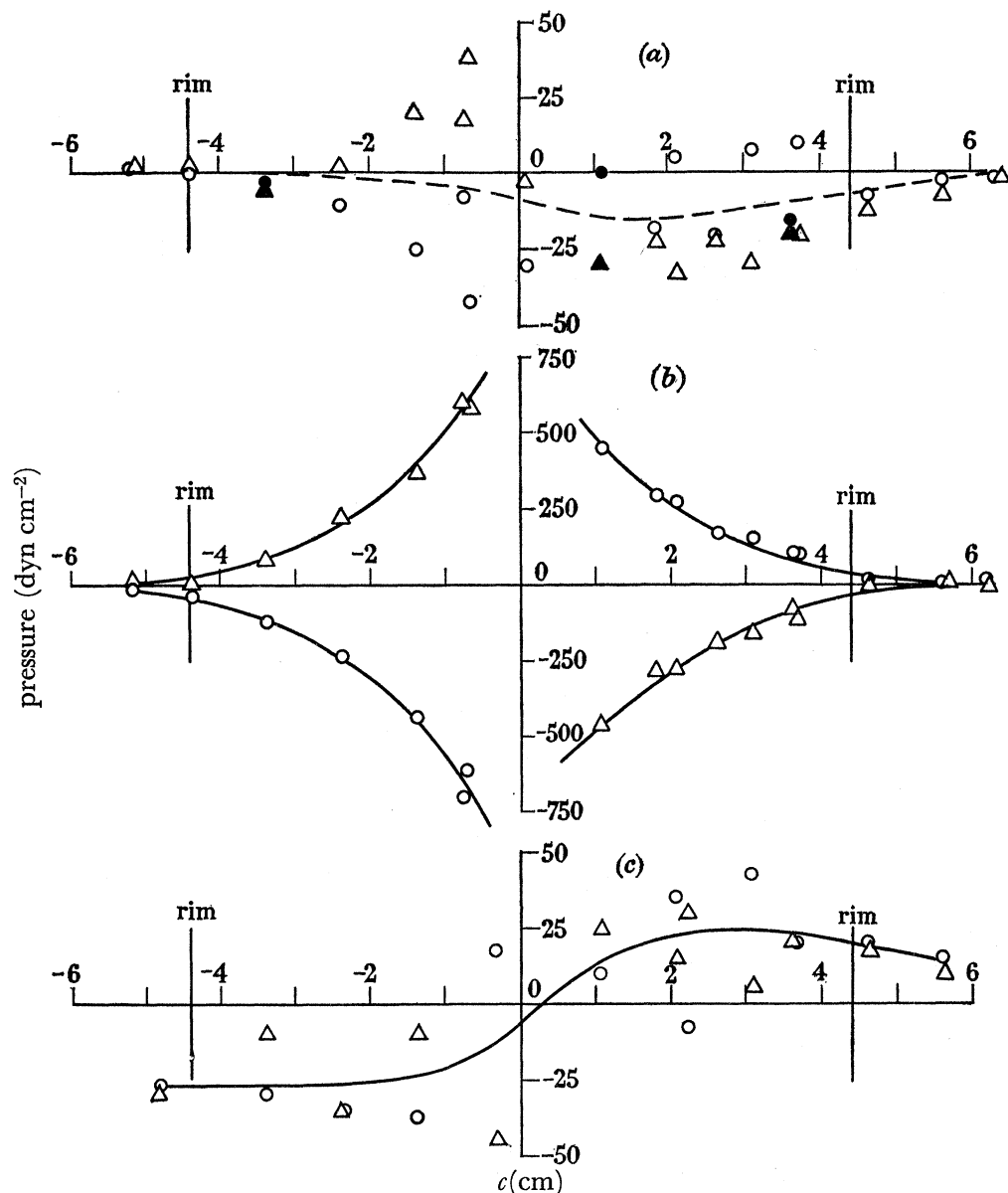


FIGURE 5. Pressure distributions when the axis of rotation is not perpendicular to the stationary plate: 3° cone-and-plate system. Legend as in figure 4, except that $\epsilon = 0.06^\circ$ in (5*b*).

In figure 5, the results of similar measurements made with the cone-and-plate system are presented. The pressure distribution along a line perpendicular to the line of greatest slope (figure 5(*b*)) has the same symmetry and displays the same change of sign on reversal of the sense of rotation as the corresponding distribution for the plate-and-plate system (figure 4(*b*)), but the greatest pressure occurs near the axis of rotation and is three times larger than the greatest pressure in figure 4(*b*) although the tilt is four times smaller; the speeds of rotation and the values of separation at the rim are the same in the two cases.

It follows that, according to these results, the wedge effect is about twelve times greater in a cone-and-plate system than in a plate-and-plate system having equal separation at the rim.

The distribution of pressure along the line of greatest slope (figure 5(c)) is similar in magnitude and form to the corresponding distribution in the plate-and-plate system (figure 4(c)).

In figures 4(a) and 5(a) the filled-in circles and triangles represent individual pressure readings taken with the three gauges when the stationary plate is adjusted so as to be as nearly perpendicular to the axis of rotation of the rotating member as possible. The open circles and triangles represent readings taken after the horizontal traverse and differential screws had been altered (in the process of taking the data of figures 4(b), (c) and 5(b), (c)) and the latter returned to the same settings as they had when the plate had been accurately alined at the outset. The pressure changes observed on reversal of the sense of rotation indicate (i) that the plate can be sufficiently well alined in a given position of the transverse for the wedge effect to be substantially eliminated; and (ii) that use of the horizontal traverse (and differential screws) can introduce a loss of alinement which gives rise to small wedge effect. Errors from the latter can be eliminated by taking the average pressure for the two senses of rotation.

The above data can be used to estimate errors which arise from the imperfections of the horizontal traverse, which give rise to a change of tilt of the order of 0.01° between the extreme positions α , γ used in obtaining the main body of data on polymer solutions. In view of the non-uniform pressure distributions of figures 4(c) and 5(c) (which are not changed in sign on reversal of the sense of rotation), and the fact that the procedure of taking the average of pressures recorded at points on opposite sides of and equidistant from the axis of rotation involves the use of the horizontal traverse, it is clear that a systematic change of tilt in the traverse will give rise to systematic error in the average pressure. However, on the reasonable assumption that the effects of figures 4(c) and 5(c) are proportional to angle of tilt and to the viscosity, it is found that the maximum value of this error is about 1 dyn cm^{-2} , and is therefore negligible. The very much greater effects of the kind shown in figures 4(b) and 5(b) are eliminated by taking the average of pressures recorded with the two senses of rotation in each position before using the horizontal traverse.

(ii) *Centrifugal forces*

The effect of centrifugal forces (supposed negligible in the theory of §2 above) on a liquid in a state of shear flow between a rotating and a stationary member is expected (a) to give rise to a slow circulatory flow radially inwards along the stationary plate and radially outwards along the rotating member, and (b) to give rise to a radial variation of pressure on both members, with a minimum on the axis of rotation. Since the pressures attributable to centrifugal forces in the present conditions are found to be small (in comparison with pressures attributable to unequal normal stress components), it is reasonable to make a correction for the pressure and to ignore the circulatory flow. For this purpose, we use the formula

$$p_{(ii)} = \frac{1}{6}\rho\Omega^2(r^2 - R^2) + p_R, \quad (4.1)$$

where $p_{(ii)}$ denotes the pressure due to centrifugal forces at a point distant r from the axis

of rotation, ρ denotes the density of the liquid, Ω the angular velocity, R the radius of the rotating member, and p_R the pressure at the rim.

This is an approximate formula, derived on the assumption that at given r , the centrifugal force at each point may be replaced by its value averaged over the gap at that value of r (Greensmith & Rivlin 1953). Derived for the parallel plate system, it can easily be shown to hold equally for the cone-and-plate system if the corresponding assumption be made that centrifugal forces may be averaged with respect to gap angle θ at given r .

By differentiating (4.1), we obtain the equation

$$r dp_{(ii)}/dr = \frac{1}{3}\rho\Omega^2 r^2. \quad (4.2)$$

Equations (4.1) and (4.2) have been used to apply corrections for centrifugal forces to the pressure and pressure gradient data reported in §5 below for polymer solutions. For the pressure gradient data, the magnitude of this correction varies from 1% or less to 11% for solution I and is less than 1% for solution II.

Measurements with the present apparatus, using a rotating cone as well as a rotating plate, have been made in order to test the validity of equation (4.1). Two liquids were used: dimethylphthalate and the silicone fluid (MS 200/1000 cS) already referred to. These have comparable densities (1.19 and 0.89 g/ml.) but very different viscosities (0.1 and 10.6 P). The data obtained (pressure as a function of radius r , at different values of Ω) are shown in figure 6, which also includes the straight line representing the theoretical relation obtained from equation (4.1) with $p_R = 0$. The rather large scatter of the experimental points is probably due to the fact that the pressures are small: the greatest pressure is 275 dyn cm⁻², while most of the pressures lie in the range 5 to 150 dyn cm⁻². A single measurement of pressure is liable to an error of about ± 5 dyn cm⁻².

These measurements were taken with the apparatus alined so that the effects of tilt (discussed in §4(a)) were either negligible or were eliminated by taking the average of pressures recorded for both senses of rotation. On the reasonable assumption that normal stress components are equal for these liquids, the pressures recorded under these conditions must be attributed to the effect of centrifugal forces. The remaining possible sources of pressure, namely (iii) and (iv) above, can be ruled out for reasons given below. The fact that the experimental points lie on the whole a little below the theoretical line in figure 6 probably arises from the approximate nature of the theory leading to equation (4.1).

(iii) *Axial movement of rotating member*

Owing to unavoidable slight imperfection in the bearing, the rotation of the shaft I (figure 1) gives rise to a very small periodic axial movement of the shaft and its attached cone or plate. This in turn gives rise to a small periodic movement of fluid in the gap between rotating and stationary members. Because the gap is small and the area of the rotating member is large, this small movement can give rise to large periodic pressures when the liquid viscosity is of the order of a few poise. For the case of flow of a Newtonian incompressible fluid of viscosity η between circular parallel plates of radius R which are instantaneously separating at speed v when the gap is h , a calculation (based on neglect of inertial forces) gives the following expression for the pressure $p_{(iii)}$ at a point distant r from the centre:

$$p_{(iii)} = -3 \frac{\eta v (R^2 - r^2)}{h^3} + p_R \quad (4.3)$$

(Stefan 1869). A similar calculation (to be published elsewhere) for the case of flow between a cone and plate leads to the approximate equation

$$p_{(iii)} = -6 \frac{\eta v}{\theta_0^3} \left(\frac{1}{r} - \frac{1}{R} \right) + p_R, \quad (4.4)$$

when θ_0 , the gap angle in radians, is small.

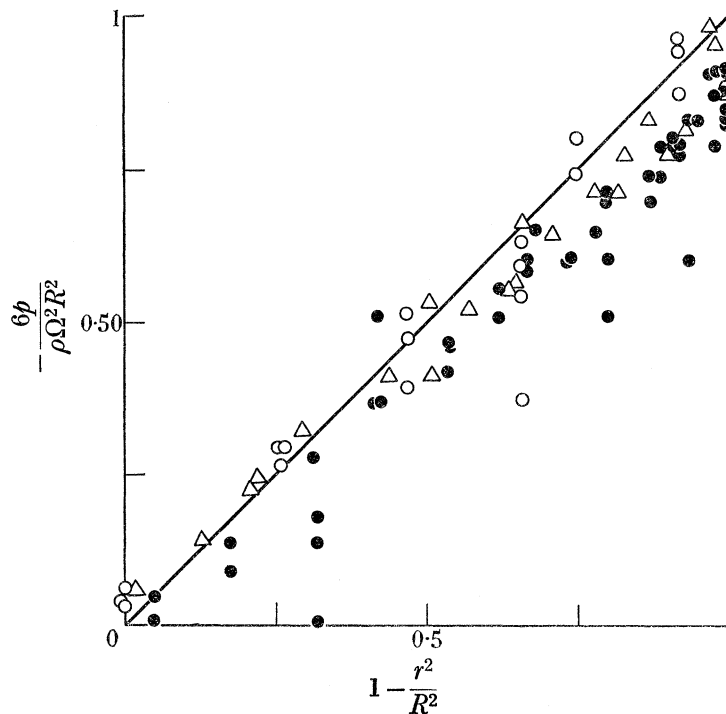


FIGURE 6. Pressures attributed to centrifugal forces. ●, Silicone fluid (10.6 P); parallel plates, 0.125 in. gap; $\Omega = 4.2$ and 6.0 rad/s. Δ , Dimethylphthalate (0.1 P); cone-and-plate, 3° gap; $\Omega = 6.8$ rad/s. ○, Dimethylphthalate (0.1 P); parallel plates, 0.100 in. gap; $\Omega = 2.2$ to 9 rad/s. —, Theory (equation (4.1) with $p_R = 0$, $p = p_{(ii)}$).

In the present apparatus, in which the velocity v derives from a periodic axial movement of amplitude Δh , say, and angular frequency Ω equal to the angular velocity of the rotating member, the maximum value of v will be $\Omega \Delta h$ if the axial movement be sinusoidal. The flow giving rise to the pressure $p_{(iii)}$ of (4.3) and (4.4) will in this case be superposed on the steady shear flow arising from the rotation, and in this respect the situation differs from that considered in the derivation of equations (4.3) and (4.4), namely, axial movement of otherwise stationary plates. To estimate the order of magnitude of pressure arising from axial movement, we shall assume that these two flows can be treated as if they were independent of one another, and accordingly that the pressure is given by (4.3) or (4.4) irrespective of the presence of the shear flow arising from relative rotation of the two members.

Using values $\eta = 10$ P, $\Omega = 10$ rad s $^{-1}$, $\Delta h = 15$ μ in., $h = 0.1$ in., $R = 4.4$ cm, $r = 2.2$ cm, gap angle = 3.23° , appropriate to the present apparatus, equations (4.3) and (4.4) give values of 10 and 50 dyn cm $^{-2}$ for the maximum values of pressure $p_{(iii)} - p_R$ in the parallel plate and cone-and-plate systems.

NORMAL STRESS DIFFERENCES IN STEADY SHEAR FLOW 167

If the viscosity η is independent of shear rate, the average value of $p_{(iii)} - p_R$ over a period of rotation will be zero, and (except for the longer periods of rotation used, when the effect will be less anyway) it is this average value which is recorded by the present pressure-measuring system whose response time is of the order 5 to 10 s. If η depends on shear rate, and if the axial movement is unsymmetric (e.g. has a saw-toothed waveform rather than a sinusoidal waveform), then it can be shown that, owing to the dependence of pressure on the product ηv in equations (4.3) and (4.4), the average value of $p_{(iii)} - p_R$ over a period is not necessarily zero. In such a case, however, the average value would be small compared with the amplitude of the pressure variation, and since this amplitude is itself small (according to the above estimate), we are justified in neglecting contributions to (average) pressure arising from axial movement of the rotating member. It should be noted, however, that owing to the dependence of this pressure on the cube of h or θ_0 , the use of appreciably smaller gaps between rotating and stationary members could give rise to pressures which are not negligible.

(iv) *Finite size of holes*

The use of liquid-filled holes in the stationary plate to measure the distribution of pressure on that plate must give rise to systematic errors in the recorded pressure values owing to the local disturbances to the state of shear flow which the holes themselves must introduce. For a viscous liquid, these disturbances may take the form of a depression of streamlines into the hole, possibly combined with a circulatory motion of otherwise stagnant liquid in the cylindrical cavity beneath the mouth of the hole. It is reasonable to assume that the flow is laminar and that the effect is primarily one of viscosity; accordingly, we may assume that for the case of a single hole in an infinite plate the associated pressure $p_{(iv)}$ depends only on the shear stress p_{21} in the undisturbed shear flow between the plates, on the gap, h , between the plates and on d , the diameter of the hole. A dimensional argument then shows that

$$p_{(iv)} = p_{21} f(d/h), \quad (4.5)$$

where f denotes an unknown (dimensionless) function. Since d/h varies with radius r in the cone-and-plate system but is independent of r in the parallel plate system, it follows that the effect of the holes could be to give a systematic difference between the radial distributions of pressure in the two systems. It is therefore of particular importance to ensure that an investigation of the kind considered in this paper is performed in conditions under which $p_{(iv)}$ is negligible. In the measurements on polymer solutions described in §5 below, the values of d/h lie in the ranges

$$\left. \begin{array}{l} 0.13 \text{ to } 0.32 \quad (\text{parallel plates}); \\ 0.20 \text{ to } 0.59 \quad (3^\circ \text{ cone-and-plate, } r \geq 1.5 \text{ cm}); \\ 0.13 \text{ to } 0.37 \quad (5^\circ \text{ cone-and-plate, } r \geq 1.5 \text{ cm}). \end{array} \right\} \quad (4.6)$$

No calculation of $p_{(iv)}$ for the case of a hole of circular cross-section appears to have been published. For the case of a hole or slit of rectangular cross-section in which one dimension is indefinitely great and the other dimension, of width d' , is parallel to the direction of the undisturbed shear flow, Thom & Appelt (1958) obtain the results

$$p_{(iv)} = 0.036 p_{21} \quad \text{and} \quad 0.13 p_{21}, \quad (4.7)$$

when $d'/h = 0.5$ and 1.0 respectively, at the very low values of Reynold's number appropriate to our experiments; the liquid is here considered to be incompressible Newtonian. It is likely that the value of $p_{(iv)}$ for a circular hole of diameter $d = d'$ will be less than the value for the slit. If so, it follows from (4.6), (4.7) that in the present series of measurements the value of $p_{(iv)}$ would be less than about 5% of the value of shear stress p_{21} .

It would be desirable to make direct measurements of $p_{(iv)}$, but this has not so far been possible with the present apparatus owing to the small diameter (0.05 cm) of the holes in the stationary plate; when the gap between parallel plates is reduced to this size (about 0.05 cm), the pressure is found to vary periodically with a large amplitude, no doubt due to the enhanced effect of the axial movement of the rotating member (equation (4.3)).

However, there is strong evidence that the effects of the holes are negligible under the conditions in which the apparatus is used. The pressure data obtained with Newtonian liquids (figure 6) have very nearly the dependence on r, Ω which is expected if these pressures arise from centrifugal forces alone; this indicates that pressures due to holes are small compared with pressures due to centrifugal forces, which are themselves small in comparison with the pressures measured in polymer solutions and attributed to normal stress differences. Furthermore, the pressures represented in figure 6 arise in conditions corresponding to a wide range of values of p_{21} , the shear stress in the undisturbed flow above the hole. To illustrate this point, the data of figure 6 on Newtonian liquids have been represented in a different way in figure 7: the ordinate is chosen in such a manner that it has the value unity whenever the measured pressure p is entirely due to centrifugal forces, supposed given by the theoretical relation (4.1) with $p_R = 0$; the abscissa represents the shear stress p_{21} . The values of d/h are also indicated in figure 7. It is seen that, for a liquid of given viscosity, there is no dependence on p_{21} ; in particular, the points for the high-viscosity liquid for the value $d/h = 0.21$ are independent of p_{21} over a range of values of p_{21} nearly equal to the range (0 to about 2000 dyn cm^{-2}) covered in the experiments on polymer solutions reported below. According to equation (4.5), this implies that $p_{(iv)}$ is negligible. Despite the scatter, it appears that, while the points for the low-viscosity liquid fall, on the average, near the horizontal line of ordinate unity, the corresponding line for the high-viscosity liquid has ordinate about 0.85. This comparatively small difference in ordinates (the viscosities differ by a factor 100) perhaps indicates that the averaging procedure used in obtaining the approximate relation (4.1) is (for some unknown reason) less reliable the higher the viscosity.

(v) *Perturbations in the state of flow*

Consideration of the compatibility of the stress equations of motion shows that for a liquid for which the value of $p_{11} + p_{22} - 2p_{33}$ in shear flow differs from zero and depends on shear rate, the state of shear flow assumed in §2(ii) between cone and plate cannot be maintained by the action of any system of external surface traction plus the forces of gravity and inertia (Oldroyd 1958). Moreover, these are just the liquids which give rise to a non-uniform pressure distribution in the cone-and-plate system (cf. equation (2.7)). In the cone-and-plate apparatus there must therefore in practice be some perturbation to the assumed state of shear flow, and this must give rise to a perturbation in the pressure distribution. An approximate calculation (to be published elsewhere) of these perturbations has led to the conclusion that the velocity perturbation is of the order of magnitude $\theta^4/320$

NORMAL STRESS DIFFERENCES IN STEADY SHEAR FLOW 169

of the greatest velocity in the unperturbed (shear) flow, and that the associated pressure perturbation $p_{(v)}$ on the plate at a point distant r from the axis of rotation is given by the equation

$$p_{(v)} = -\frac{\theta_0^2}{20} (p_{11} + p_{22} - 2p_{33}) \ln \frac{r}{R} + p_R, \quad (4.7)$$

where $p_{11} + p_{22} - 2p_{33}$ is the value in the unperturbed (shear) flow and θ_0 is the gap angle in radians.

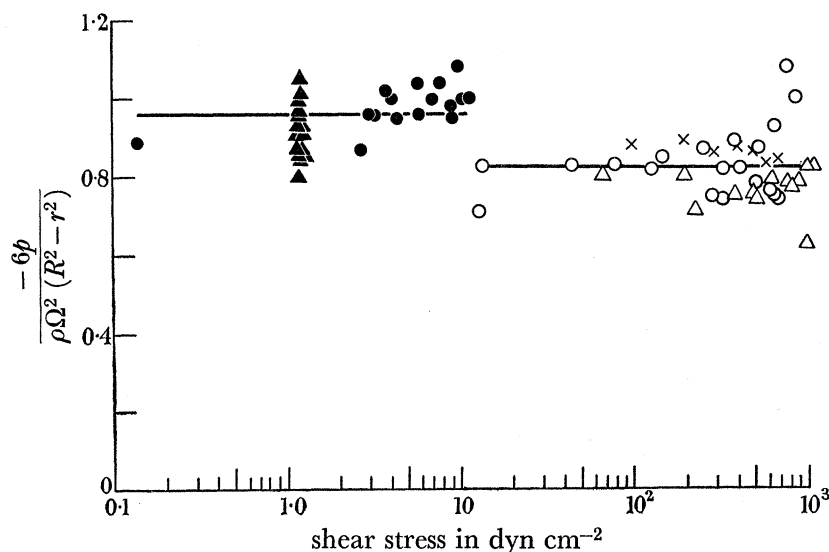


FIGURE 7. Search for pressure contribution due to hole size. Silicone fluid (10.6 P), $\Omega = 5.96$ rad/s, parallel plates: $d/h = 0.16$ (\times), 0.21 (\circ), 0.32 (\triangle). Dimethylphthalate (0.1 P): parallel plates, $d/h = 0.20$; $5.6 \leq \Omega \leq 8.97$ (\bullet); 3° cone-and-plate, $0.27 \leq d/h \leq 1.62$, $\Omega = 6.8$ (\blacktriangle).

It follows that $p_{(v)}$ has the same dependence on r as has the pressure arising from the difference of normal stress components in (unperturbed) shear flow but, in contrast to this pressure, depends (at a given shear rate) on the gap angle θ_0 . The agreement found (figure 10a) between pressures recorded at constant shear rate for solution I with different values of θ_0 thus shows that $p_{(v)}$ is negligible in the present experiments. This is consistent with the fact that the value of the coefficient $\theta_0^2/20$ in (4.7) is very small (1.3×10^{-4} and 4×10^{-4} for the 3° and 5° cones). The rather less good agreement with solution II (figure 10b) is discussed below.

No similar perturbation arises in the flow between parallel plates; if inertial forces are neglected, the assumed state of shear flow §2 (iii) can be maintained by the action of external surface tractions alone.

5. PRESSURE MEASUREMENTS WITH TWO POLYMER SOLUTIONS

(a) Preparation and composition of solutions

Solution I contained 5.76 g of polyisobutylene of number-average molecular weight 10^6 (L100 from Esso Ltd) in a 100 ml. of dekaline; it was used throughout the pressure measurements at a temperature of 22.0°C . In order to remove insoluble impurities, the polymer was first dissolved in benzene, the solution filtered, the polymer re-precipitated with methanol and dried in a vacuum oven. From a master batch of concentrated solution

containing 12 g of polymer in 100 ml redistilled dekalin (dissolution being effected by slow rotation in a tilted flask for 1 or 2 weeks at 60 °C), the solution used in the measurements was prepared by dilution of a sample.

Solution II contained 2.44 g of polymethylmethacrylate of number-average molecular weight 10^6 (obtained from I.C.I. Ltd. Plastics Division) in 100 ml. dimethyl phthalate; it was used throughout at a temperature of 24.2 °C. The solution was prepared by adding the polymer in a finely divided form to the solvent; the mixture was rotated slowly in a tilted flask for a few days at 60 to 70 °C. The solution, before use, was filtered through a sintered glass filter (grade no. 1).

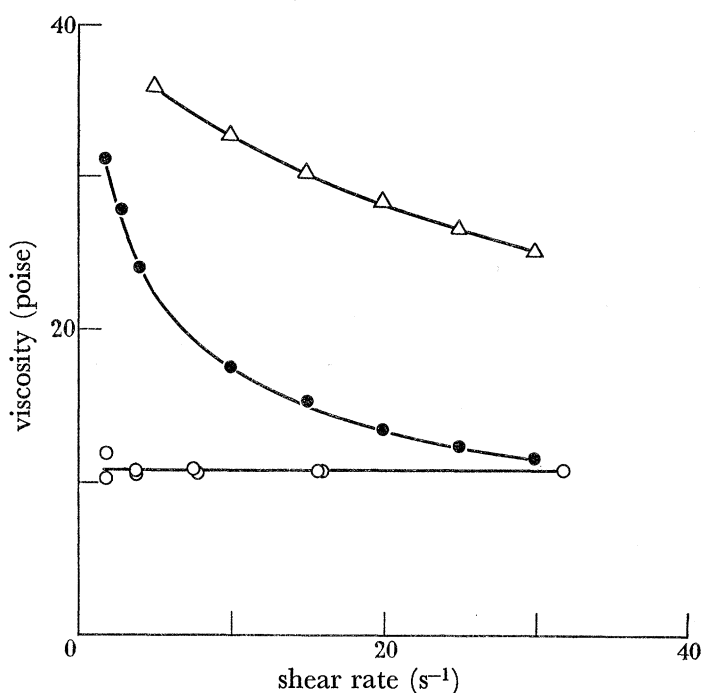


FIGURE 8. Viscosity as a function of shear rate. — Δ —, Solution I, 23 °C; — \bullet —, solution II, 24 °C; — \circ —, silicone fluid, 24 °C.

The viscosities of solutions I and II and of the silicone fluid used in the investigation of tilt (§ 4) were measured at several shear rates in a concentric cylinder apparatus constructed by Saunders & Kaye (in course of publication). The results are given in figure 8. Solution II was highly elastic when judged qualitatively by the recoil of small air bubbles observed when a rotating container of the solution was suddenly brought to rest; solution I was less elastic, while the silicone fluid was inelastic.

(b) *Pressure changes at the start of shear flow*

It is found that the two polymer solutions used here behave very differently in regard to the transient changes of pressure which are observed when the upper member is first made to rotate at constant speed (figure 9). The pressure (at a given value of r) in the case of solution I rises at once to its steady value. In the case of solution II, however, the pressure rises at a finite rate, passes slowly through two pronounced maximum values, and after about an hour's rotation reaches a more-or-less steady value; if the rotation is then stopped

NORMAL STRESS DIFFERENCES IN STEADY SHEAR FLOW 171

for a few seconds and switched on again, the maxima do not reappear, but increasing periods of rest lead to a reappearance of and a progressive increase in the pressure maxima.

Since these measurements are taken with the apparatus aligned as accurately as possible, it follows that, in the light of the discussion of other sources of pressure given in §4 above, the recorded variations of pressure with time must be attributed to a similar variation of

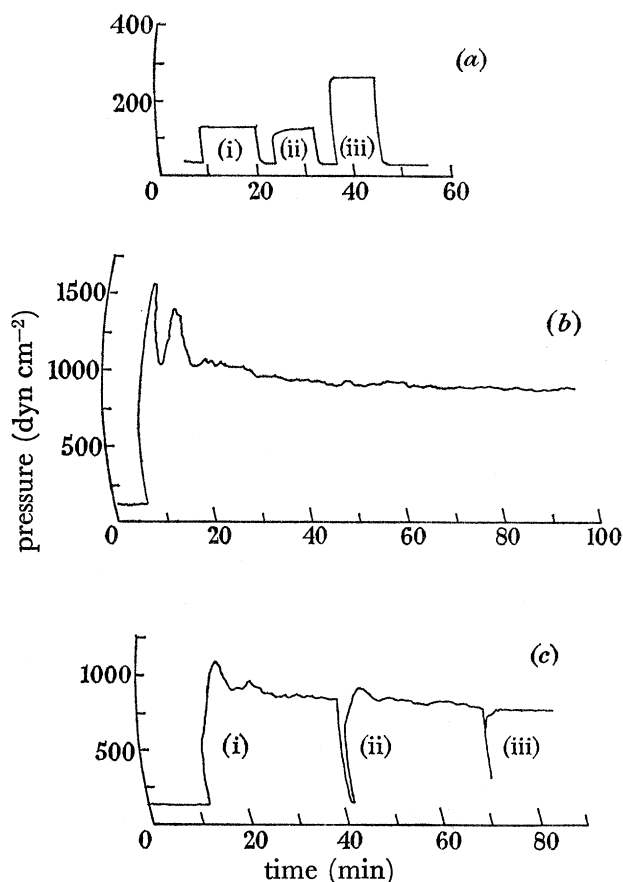


FIGURE 9. Pressure changes at the start of shear flow. (a) Solution I: shear rate 22 s^{-1} , clockwise (i) and anti-clockwise (ii) rotation; shear rate 42 s^{-1} (iii). $r = 2.56 \text{ cm}$. (b) Solution II: shear rate 23 s^{-1} , after 16 h rest. 3° cone; $r = 2.56 \text{ cm}$. (c) Solution II: shear rate 23 s^{-1} , after rest periods of 1 h (i), 1 min (ii) 6 s (iii). 3° cone; $r = 2.56 \text{ cm}$. The zero position on the pressure scale is arbitrary.

differences of normal stress components with time. This must presumably be attributed to some change with time of whatever long-chain molecular structure in the solution it is which gives rise to differences in normal stress components. A liquid whose rheological properties change reversibly during prolonged flow is sometimes called 'thixotropic', although this term has been used in other ways. The phenomenon is well-known in relation to changes of shear stress with time of shearing, and has recently been reported for normal stress differences by Trapeznikov, Morozov & Petrzhih (1960) who measure total thrust and torque in a cone-and-plate apparatus using liquids containing aluminium naphthenate. It is interesting to note that they, too, have found a double maximum in the total thrust; the occurrence of a second maximum would seem more difficult to explain than the occurrence of a single maximum.

It is important to note that there is some evidence to show that the structural changes which solution II apparently undergoes during the first 30 min shearing are accompanied by the growth of heterogeneities of a size (about $\frac{1}{2}$ mm) comparable with the gap between stationary and rotating members (Lodge 1961 *b*). This must lead to a breakdown of assumptions (ii), (iii) and (v) of §2 above relating to the state of flow in the gap and the sole dependence of normal stress differences on shear rate. For this reason, values of normal stress differences derived below from pressure measurements in the case of solution II cannot be regarded with great confidence. These measurements are made after sufficient time has elapsed for the pressures to reach steady values; the use of the horizontal traverse brings into the gap some solution which has previously been at rest, but this is also allowed sufficient time of shearing in each case for the pressures generated to reach steady values.

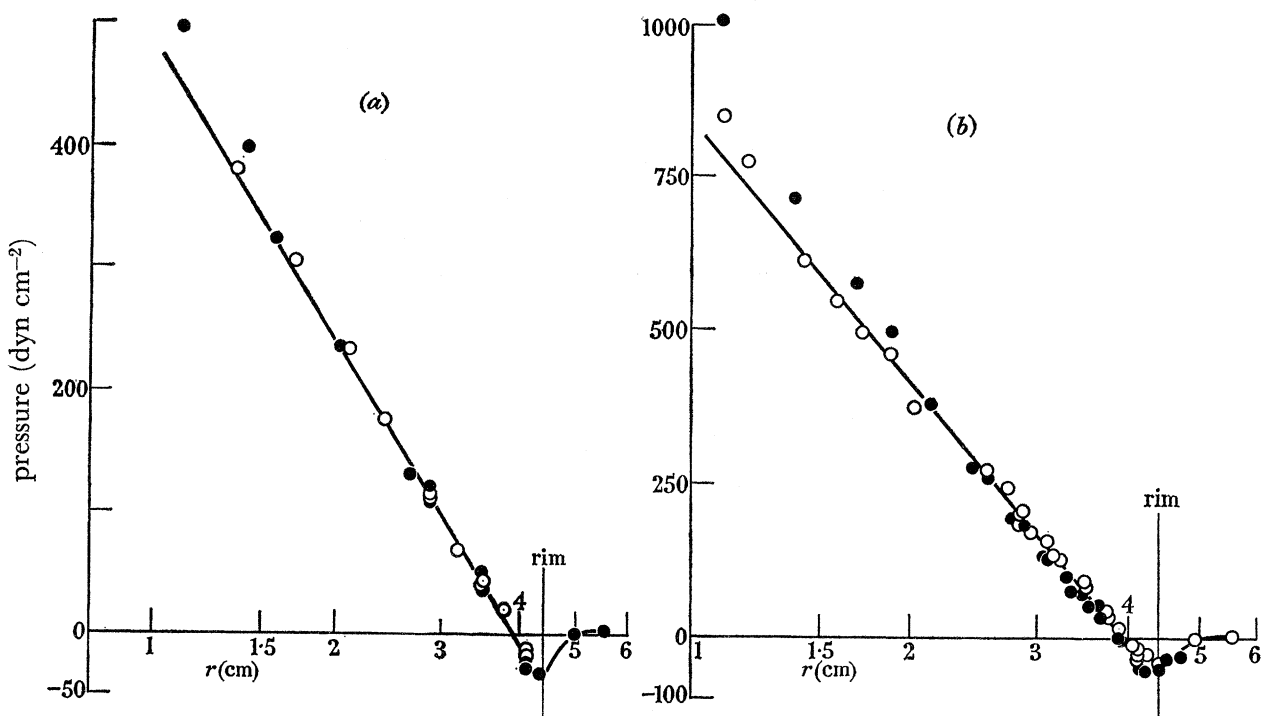


FIGURE 10. Pressure distributions in cone-and-plate system with different gap angles. (a) Solution I, shear rate 22.8 s^{-1} , (b) solution II, shear rate 10.8 s^{-1} . Gap angles 5.17° (\circ), 3.23° (\bullet). Each point represents the value of $\bar{p} + p_{(ii)}$, where \bar{p} is the mean pressure for two senses of rotation taken with the cone rotating in a sea of liquid, and $p_{(ii)}$ is the centrifugal correction calculated from equation (4.1) with $p_R = 0$. The horizontal scale is logarithmic.

(c) *Pressure distributions with different gaps*

From the arguments of §2 above relating to equations (2.7) and (2.9), it follows that at any given value of r the pressure gradient ($-r dp_{22}/dr$) depends only on the local value of shear rate; if, therefore, the gap or gap angle be altered, with alteration of rotation speed so as to maintain a constant shear rate at given r , the pressure gradient at each r -value, and hence also the form of the pressure distribution, will be unchanged. There may be a change in the level of the pressure distribution, because the absolute value of pressure at given r will depend on the value of the pressure near the rim and this may change because it

presumably will depend on the more complicated state of flow near the rim of the rotating member.

Pressure distributions at constant shear rate recorded using the cone-and-plate system with two gap angles are shown in figure 10 and using the parallel plate system with three gaps in figure 11. It is seen that the results for solution I (figures 10(a) and 11(a)) are in agreement with expectation; furthermore, the pressure in the cone-and-plate system varies linearly with $\log r$ (in agreement with (2.7)) over the outer half of the gap

$$(2 \text{ cm} \leq r \leq 4.4 \text{ cm}).$$

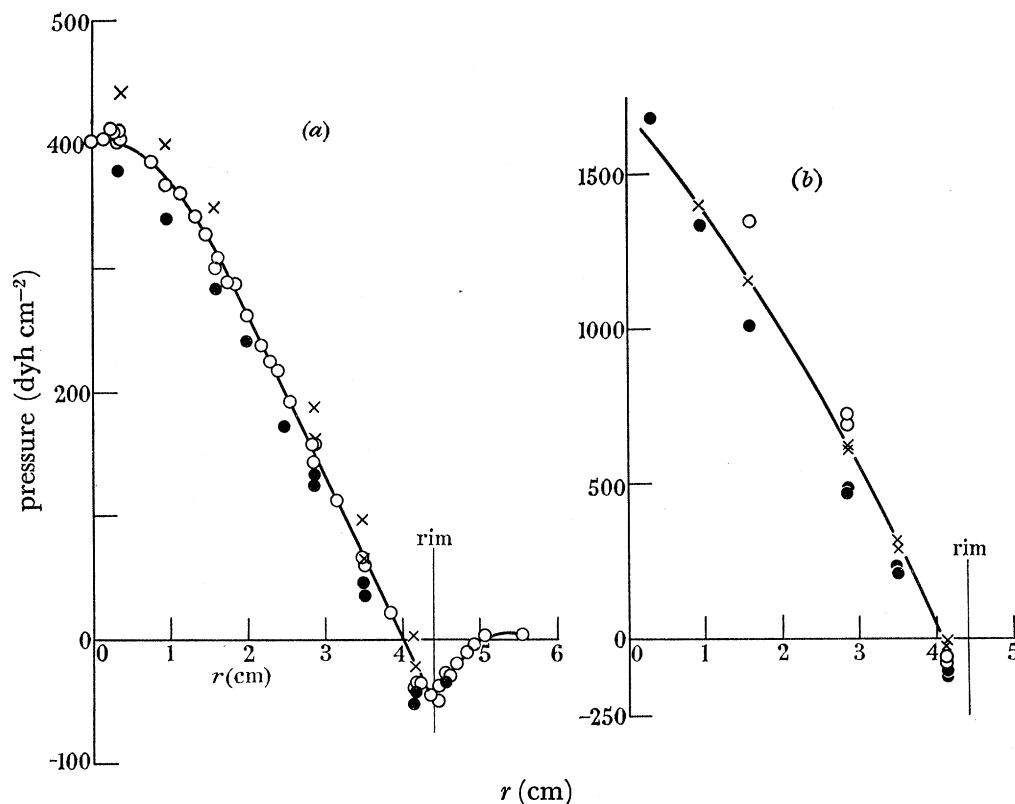


FIGURE 11. Pressure distributions in the parallel plate system with different gaps. (a) Solution I, shear rate 25.7 s^{-1} at $r = 3.5 \text{ cm}$. (b) Solution II, shear rate 20.5 s^{-1} at $r = 3.5 \text{ cm}$. Gap 0.06 in . (●), 0.100 in . (○), 0.150 in . (×). Each point represents the value of $p_{(tl)} + p$ taken with the plate rotating in a sea of liquid.

The departure from this relation observed in the inner half of the gap ($r < 2 \text{ cm}$) may, if significant, be due to an effect of the hole, since the gap in this region is comparable to the hole diameter (for the 3° cone, the hole diameter and gap are equal when $r = 0.9 \text{ cm}$). In the parallel plate system (figure 11(a)), the level of the pressure distribution depends on the size of the gap but the form and gradient do not.

The corresponding results for solution II are less satisfactory, for the pressure gradient in the parallel plate system (figure 11(b)) is seen to depend on the size of the gap, even in the outer half of the gap ($r > 2 \text{ cm}$). This is a second reason for not placing great weight on the results obtained with solution II.

Further results obtained using the above gaps and gap angles are represented in figure 12.

(d) Pressure gradients at various shear rates

In figure 12 are presented the values of pressure gradient, $r dp_{22}/dr$, derived from pressure distribution data of the type shown in figures 10, 11, for various values of shear rate. In most cases, the pressure gradient is calculated from mean pressures at two values of r (2.86 and 4.13 cm); each of these mean pressures is the mean of four single pressure readings taken with two gauges (A , B) and two senses of rotation. A correction for centrifugal forces is made as described above, using equation (4.2).

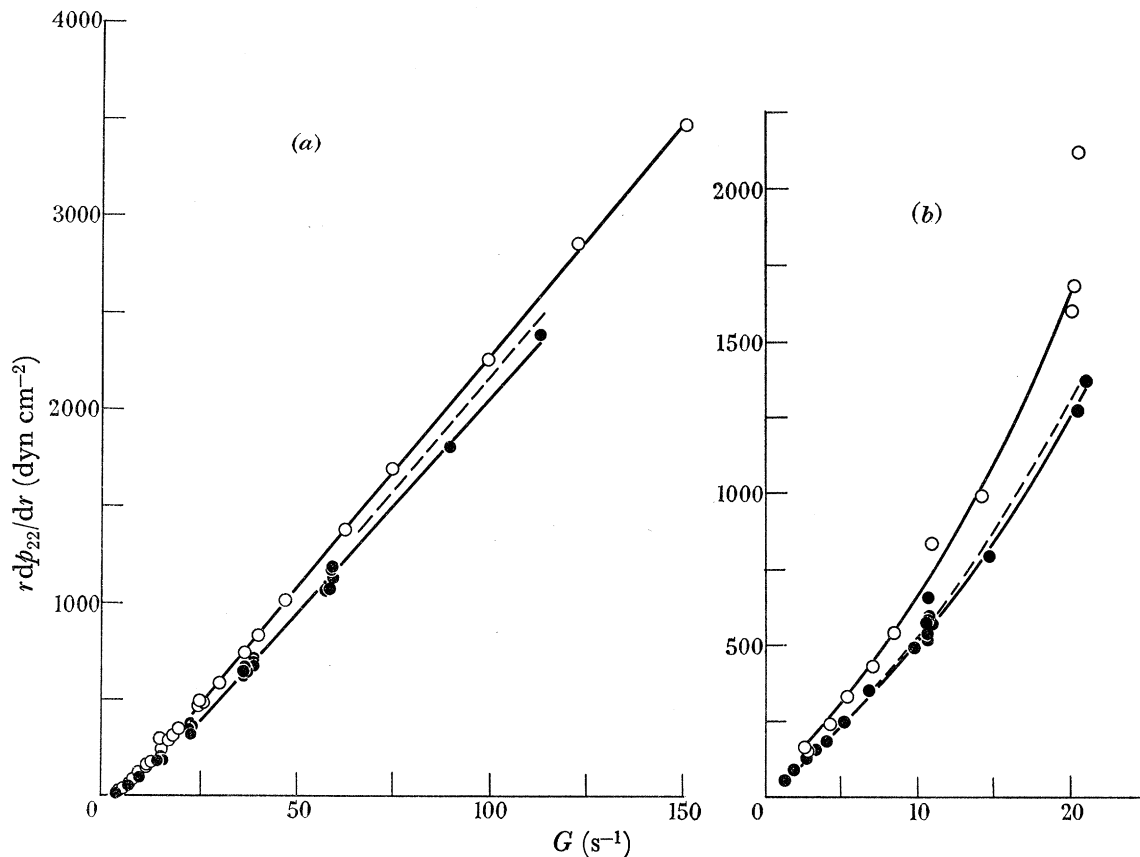


FIGURE 12. Pressure gradients in cone-and-plate and parallel plate systems at various shear rates. \circ , Parallel plate system (0.15 in., 0.10 in., 0.06 in. gaps; sea of liquid); \bullet , cone-and-plate system (3.23° , 5.17° gap angles; with and without sea of liquid). (a) Solution I; the full lines are those fitted by least squares in the range $15 < G < 151$. (b) Solution II. Broken lines are obtained by adding $(1 - Gd/dG) p_R$ to ordinates of lower full curves. Each point (\circ , \bullet) is obtained from eight single pressure readings taken with gauges A , B at positions $r = 2.86$ cm, 4.13 cm (when sea of liquid is used) and two senses of rotation, a correction being made for centrifugal forces.

The data presented in figure 12 are perhaps the most important in this paper. In the first place, according to equation (2.7), the data for the cone-and-plate system must represent the value of $p_{11} + p_{22} - 2p_{33}$ (one combination of the required normal stress differences) as a function of shear rate. In the second place, the fact that the points for the cone-and-plate system and the parallel plate system fall on two distinct curves implies that

$$p_{22} - p_{33} \neq 0, \quad (5.1)$$

for if $p_{22} - p_{33}$ were zero, equation (2.10) shows that rdp_{22}/dr would (at any given shear rate) have the same value in both systems, i.e. that points such as those of figure 12 would fall on a common curve. The difference between the curves for solution I (figure 12(a)), though apparently not large, is highly significant: for the range $15 < G \leq 151$ ($G =$ shear rate (sec^{-1})), an analysis of variance (based on the assumption that the ordinate errors are normally distributed and the abscissa errors are zero) shows that straight lines fitted by the method of least squares to the cone-and-plate and parallel plate data are significantly different at a level which is considerably better than 0.1%. For solution II (figure 12(b)), no analysis of variance has been made, but the difference between the curves appears to be equally significant, for although the scatter is greater, the relative difference of ordinates is greater too.

For solution I, the straight lines fitted to the pressure gradient-shear rate data of figure 12(a) have the following equations:

$$\left. \begin{aligned} (rdp_{22}/dr)_{pp} &= 24.1G - 132 & (15 < G \leq 141), \\ (rdp_{22}/dr)_{cp} &= 22.3G - 177 & (22 < G < 114), \end{aligned} \right\} \quad (5.2)$$

when p_{22} is in dyn cm^{-2} and G is in sec^{-1} .

In view of the provisional nature of these investigations (the taking of data was not statistically planned) and the statistical complexity associated with the fact that each point in figure 12 involves eight single pressure readings, it is considered that the present data do not merit a more detailed statistical analysis such as would be required to give (for example) confidence limits for the numbers in equations (5.2).

(e) *The value of $p_{22} - p_{33}$*

The value of $p_{22} - p_{33}$ at a given shear rate G can, according to equation (2.11), be obtained from the data of figure 12 by integrating the difference of ordinates divided by the square of the abscissa.

For solution I, this integration can be performed analytically for part of the range of integration ($G \geq 24$, say) using the empirical formulae (5.2). For the remainder of the range of integration ($0 \leq G \leq 24$), the data of figure 12a have been replotted, after division by G^2 , in figure 13a; the required integral is given by the area between the two curves so obtained. It is seen that the points of figure 13a exhibit considerable scatter and that there is some uncertainty as to where the curves representing the data are to be drawn; moreover, the extrapolation of these curves to $G = 0$ also introduces uncertainty because the ordinates at low values of G are dependent on G . On the other hand, pressures recorded in the parallel plate system (gap 0.100 in., speed 0.30 rev/s) were found to vary linearly with r^2 in the region $0 \leq r \leq 2$; this implies that rdp_{22}/dr varies linearly with G^2 in the range $0 \leq G \leq 15$; the constant of proportionality in this linear relation leads to a value for $G^{-2}rdp_{22}/dr$ which is represented by the horizontal line in figure 13a. This line is seen to disagree with the other points (represented by open circles) in figure 13a, which are obtained from pressures recorded using larger values of r and lower speeds of rotation. The reason for this disagreement is not known. For these various reasons, the present data do not enable us to determine the value of $p_{22} - p_{33}$ as a function of G with any reliability. For the sake of obtaining an estimate of the order of magnitude of $p_{22} - p_{33}$, however, the full curves have been drawn

in figure 13*a* and the area enclosed between them and the vertical lines $G = 0, 24$ has been determined graphically. The values obtained for $p_{22} - p_{33}$ from this area and from equations (5.2) (with the use of equations (2.11)) are represented by the full curves in figure 14*a*. The importance of obtaining a reliable integration at low shear rates is emphasized by the broken line in figure 14 which represents the contribution (at higher shear rates) to the value

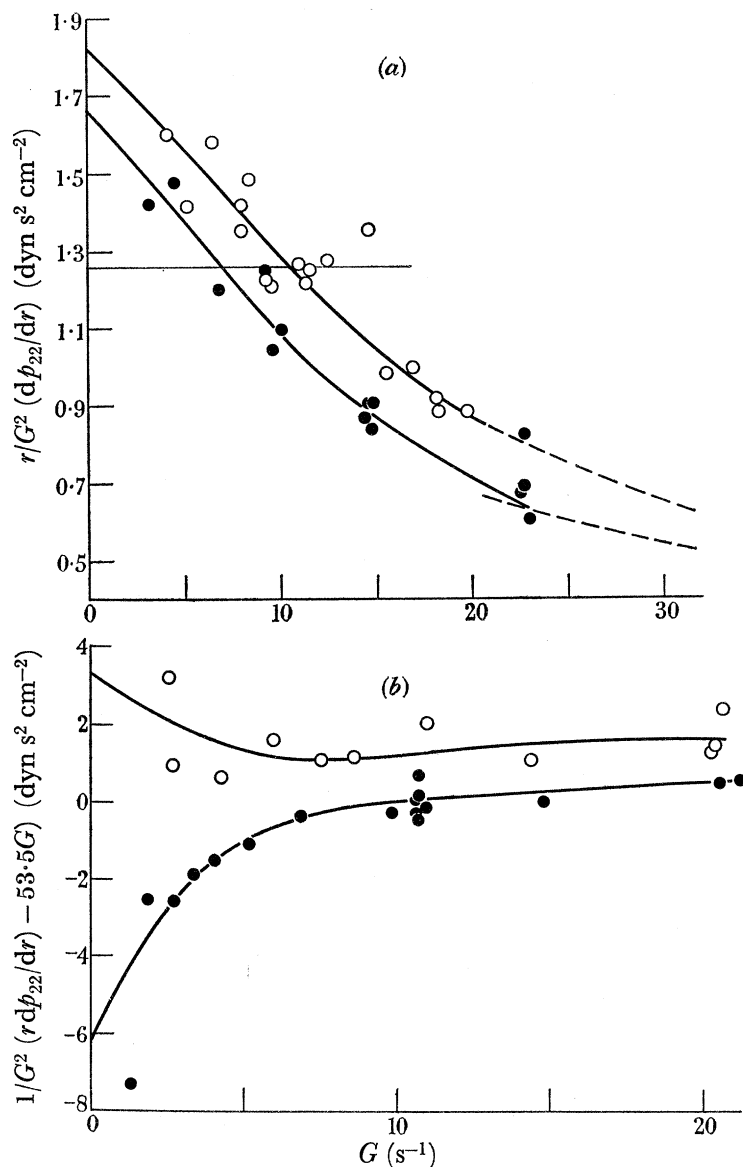


FIGURE 13. Curves used in the evaluation of $p_{22} - p_{33}$ by integration. \circ , Parallel plate system; \bullet , cone-and-plate system. (a) Solution I. The broken curves represent the 'least-squares' lines of figure 12*a*. The horizontal line is obtained from the slope of a line representing p as a function of r^2 for data at $r \leq 2$ in the parallel plate system. (b) Solution II.

of $p_{22} - p_{33}$ which is made by the term in equation (2.11) involving integration in the range $0 \leq G \leq 24$. It is the factor G outside the integral in (2.11) which is responsible for the importance of these low-shear-rate contributions to the value of $p_{22} - p_{33}$ at high shear rates.

In the treatment of data for solution II, graphical integration is used over the whole range of shear rate, no empirical equations corresponding to (5.2) having been obtained.

NORMAL STRESS DIFFERENCES IN STEADY SHEAR FLOW 177

If the data for solution II are plotted as in figure 13 (a), it is found that as G decreases, the ordinate $G^{-2}rdp_{22}/dr$ increases too rapidly to enable the integration to be carried out conveniently; accordingly, an arbitrary line ($y = 53.5G$) is drawn so as to separate, as far as possible, the ordinates rdp_{22}/dr of points for parallel plate and cone-and-plate systems in figure 12 (b), and then, in figure 13 (b), the values of $G^{-2}(rdp_{22}/dr - y)$ are plotted as

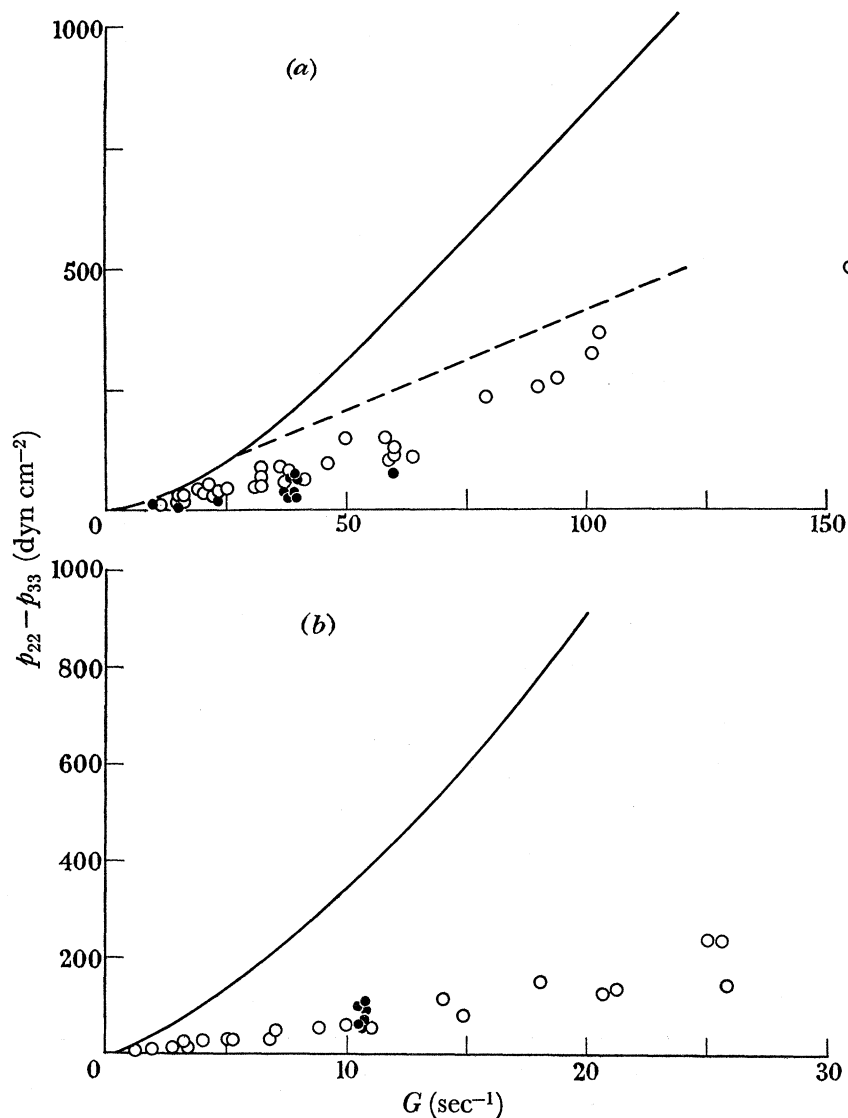


FIGURE 14. Values obtained for $p_{22} - p_{33}$ by two methods. —, From pressure gradients by integration; the broken line in (a) represents the contribution from the range $0 \leq G \leq 24$. The points represent values of rim pressure $\times (-1)$ with (○) and without (●) a sea of liquid. (a) Solution I. (b) Solution II.

ordinates for the two systems. The required integral in (2.11) is given by the area between the two curves in figure 13 (b), because the extra term $G^{-2}y$ in each ordinate cancels when the difference of ordinates for the two systems is taken. It will be seen that the extrapolation to zero shear rate which is involved in drawing the full curves in figure 13 (b) involves even greater uncertainty than that of figure 13 (a) (solution I), because as G decreases the difference of ordinates in figure 13 (b) increases. The values of $p_{22} - p_{33}$ obtained from

graphical integration of the area between the full curves of figure 13 (*b*) (by the use of (2.11)) are represented in figure 14 (*b*).

It is natural to inquire whether the values for $p_{22} - p_{33}$ so obtained from pressure gradients in the two systems agree with the values of $-p_R$, where p_R is the pressure on the plate in either system at the rim of the rotating member; according to equation (A 10) (Appendix), these should be equal when the free boundary has the shape of the surface of a sphere of radius R . A few measurements have been made using the auxiliary sharp-edged plate as shown in figure 3 to give a free liquid boundary as near to the required spherical shape as possible. Pressures so obtained using the rotating cone are shown in figure 15, which represents the results of two replications out of six made with solution II. Similar results are

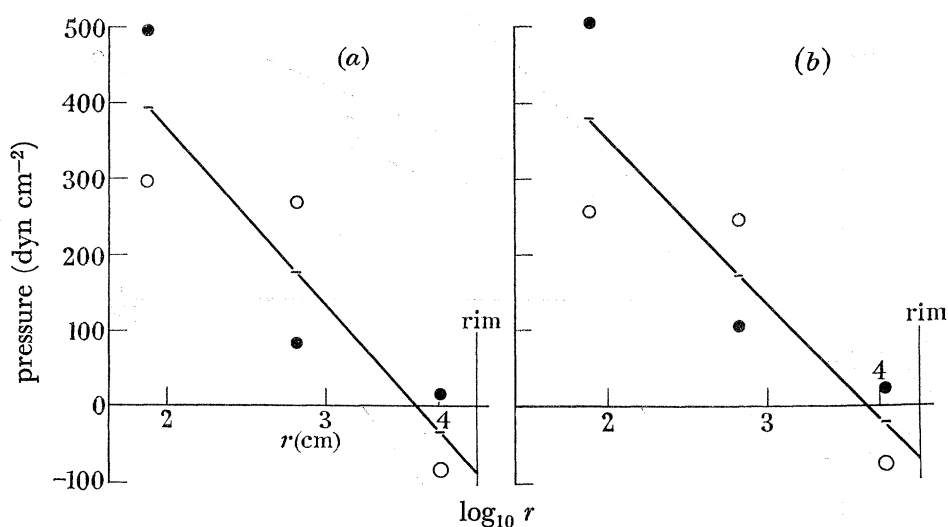


FIGURE 15. Pressure distribution when the liquid is confined to the gap between cone and sharp-edged plate. Solution II, shear rate 10.7 s^{-1} , 5° cone. The circles represent individual pressure readings for clockwise (\circ) and anti-clockwise (\bullet) rotation. The lines drawn through the means ($-$) of these readings have a negative intercept at the rim.

obtained with solution I. It is seen that, while the pressure changes as the sense of rotation is changed, the average of these pressures when plotted as a function of $\log r$ lie on a straight line in accordance with theory. The intercept of this line at the rim gives the required value of p_R , which is seen to be negative. The values of p_R so obtained, together with other values of p_R obtained using both cone-and-plate rotating in a sea of liquid, are represented by the individual points in figure 14. It is seen that, in relation to the considerable scatter of the points, there appears to be no significant difference between values of p_R obtained with and without a sea of liquid—a rather surprising result.

The values of $-p_R$ are positive and increase with increase of shear rate. They are, however, considerably smaller in value than the values of $p_{22} - p_{33}$ obtained from pressure gradients in the two systems (figure 14). The two methods of determining $p_{22} - p_{33}$ thus lead according to the present data, to discordant results. It could be argued that this is due to the uncertainty arising from the extrapolation to zero shear rate made in the integration over differences of pressure gradients, but in fact this admitted uncertainty does not resolve all or even most of the disagreement, as the following argument shows. The need for extrapolation

NORMAL STRESS DIFFERENCES IN STEADY SHEAR FLOW 179

to zero shear rate arises with the use of equation (2.11) which is obtained by integrating the differential equation (2.10). If, however, we use the values of p_R to determine $p_{22} - p_{33}$ as a function of G , the left-hand side of equation (2.10) can be evaluated (without integration), and compared with the right-hand side, whose values are given by the difference of ordinates in figure 12. The data, when treated in this way, are found to disagree with equation (2.10); the extent of this disagreement can be gauged from the broken lines in figure 12 which represent values of $(r dp_{22}/dr)_{cp} - (G dp_R/dG - p_R)$ and which would (by (2.10) and (A 10) in the Appendix) coincide with the upper full lines in figure 12, if there were no disagreement. This comparison of the determinations of $p_{22} - p_{33}$ involves no extrapolation.

The data obtained using the sharp-edged plate (figure 15) are also used to obtain values for the pressure gradient; these have been included with values obtained using a sea of liquid in figure 12. No significant difference is found between values of pressure gradient obtained with and without a sea of liquid.

6. DISCUSSION

The consideration of unwanted sources of pressure (§4) and the internal consistency of data obtained (with solution I, at least) using different gaps and gap angles (§5, figures 10, 11) offer justification for believing that the apparatus does (as intended) enable one to measure pressure distributions due solely to differences of normal stress components in steady shear flow. The departure at low values of r from the theoretical linear relation between pressure and $\log r$ in the cone-and-plate system (figure 10) is somewhat disquieting, and calls for more extensive investigation. A more extensive investigation of the effect of changing gap angle and gap size is also called for in view of its importance in verifying that the state of flow is one of shear flow.

The pressure distributions observed with the present apparatus exhibit the same main features as those observed by other workers using various liquids (Roberts 1957; Greensmith & Rivlin 1953; Kotaka, Kurata & Tamura 1959): the pressure is greatest near the axis of rotation and decreases steadily towards the rim of the rotating member. The negative values observed for the pressure at the rim accord with the observations of Greensmith & Rivlin, but not with the observations of Roberts, who reports zero values for the pressure at the rim for each of a variety of liquids investigated. In this respect, our observation of negative pressures at the rim (figure 15) when there is no sea of liquid is of particular interest because these conditions would appear to conform more closely to those of Roberts's experiments than to those of Greensmith & Rivlin's experiments.

The present experiments lead to the conclusion that $p_{22} - p_{33}$ is significantly different from zero and increases with rate of shear. This conclusion conflicts with the predictions of a phenomenological theory (Weissenberg 1947) and a molecular theory (Lodge 1956). The values obtained for $p_{22} - p_{33}$ from the two types of data used here (pressure gradients in cone-and-plate and parallel plate systems; pressures at the rim) do not agree with one another. It is not possible at present to do more than speculate as to the reasons for this disagreement. If, on the one hand, the assumptions underlying the deduction of $p_{22} - p_{33}$ from the pressure gradients are valid, then it would appear that the rim pressures cannot be used to evaluate $p_{22} - p_{33}$, presumably because the pressures arising from disturbances to the state of shear flow near the rim of the rotating member cannot be neglected; if this is the

case, however, it would be reasonable to expect to find an appreciable difference between the values of rim pressure observed when the system is used with and without a sea of liquid; no appreciable difference is in fact found, although it must be admitted that the scatter of points is rather large in these experiments. Furthermore, the values of $p_{22} - p_{33}$ derived from pressure gradients are rather large in relation to the values of $p_{11} + p_{22} - 2p_{33}$ (obtained from the pressure gradient in the cone-and-plate system) and these two sets of values taken together in fact yield values for $p_{11} - p_{22}$ which, as the shear rate is increased, at first increase and then pass through a maximum and finally decrease, reaching negative values in the case of solution II. This is a rather curious (though not impossible) result: it would imply a similar variation with shear rate in the total thrust in a cone-and-plate system (unless disturbances to the state of flow at the rim are sufficient to vitiate the argument relating total thrust and $p_{11} - p_{22}$, cf. equation (A 14) in the Appendix), whereas such published observations as there are in all cases give a total thrust (in steady conditions) which increases steadily with shear rate. If, on the other hand, we are to reject the derivation of $p_{22} - p_{33}$ from pressure gradient data, it would appear that this could be done only by rejecting assumption (v) of §2 and concluding that the normal stress differences in steady shear flow depend not only on the value of shear rate at a point but also on values of the spatial gradients of strain and hence on the curvature of the shearing surfaces and the lines of flow. Such a conclusion could in fact also account for the departures from the linear relation between pressure and $\log r$ observed with the cone-and-plate system. However, the present data would appear to be too sparse to allow a definite conclusion to be reached on this point.

APPENDIX: THE CONE-AND-PLATE SYSTEM

(a) *Conditions at a free liquid boundary*

Let us consider the case in which the free liquid boundary is confined to the gap between cone and plate, is a surface of revolution about the axis of rotation of the cone, and has a cross section of arbitrary shape in a vertical section through the axis of rotation (figure 16).

At any point O on the free boundary let us set up a local rectangular Cartesian co-ordinate system $Ox_1x_2x_3$ in which Ox_3 lies along the line VO , where V is the cone vertex; Ox_2 lies in the vertical plane (through O) and Ox_1 is horizontal, and therefore tangential to the liquid surface at O . If we ignore the effects of surface tension, the traction across the liquid boundary must be normal to that boundary and equal to the atmospheric pressure p_0 say. This gives the equations

$$p_{21} \sin \alpha + p_{31} \cos \alpha = 0, \quad (\text{A } 1)$$

$$p_{22} \sin \alpha + p_{32} \cos \alpha = -p_0 \sin \alpha, \quad (\text{A } 2)$$

$$p_{23} \sin \alpha + p_{33} \cos \alpha = -p_0 \cos \alpha, \quad (\text{A } 3)$$

where p_{ij} are the stress components referred to $Ox_1x_2x_3$ and α is the inclination of the boundary normal ON to Ox_3 . The last two of these equations are equivalent to the equations

$$(p_{22} - p_{33}) \sin 2\alpha = 0, \quad (\text{A } 4)$$

$$p_0 + p_{22} = (p_{22} - p_{33}) \cos^2 \alpha - p_{32} \sin 2\alpha. \quad (\text{A } 5)$$

Let us now suppose that the state of shear flow assumed in §2(ii) persists right up to the free liquid boundary and to the point O in particular. The axes $Ox_1x_2x_3$ then coincide with

NORMAL STRESS DIFFERENCES IN STEADY SHEAR FLOW 181

those introduced in §2(iv), the stress components p_{ij} satisfy equation (2.1), and hence the boundary conditions (A 1, 4, 5) take the form

$$p_{21} \sin \alpha = 0, \quad (\text{A } 6)$$

$$(p_{22} - p_{33}) \sin 2\alpha = 0, \quad (\text{A } 7)$$

$$p_0 + p_{22} = (p_{22} - p_{33}) \cos^2 \alpha. \quad (\text{A } 8)$$

If the free boundary is part of a sphere whose centre is at V , then $\alpha = 0$ (for all positions of O on the free boundary), equations (A 6, 7) are satisfied, and (A 8) becomes

$$p_0 + p_{22} = p_{22} - p_{33}. \quad (\text{A } 9)$$

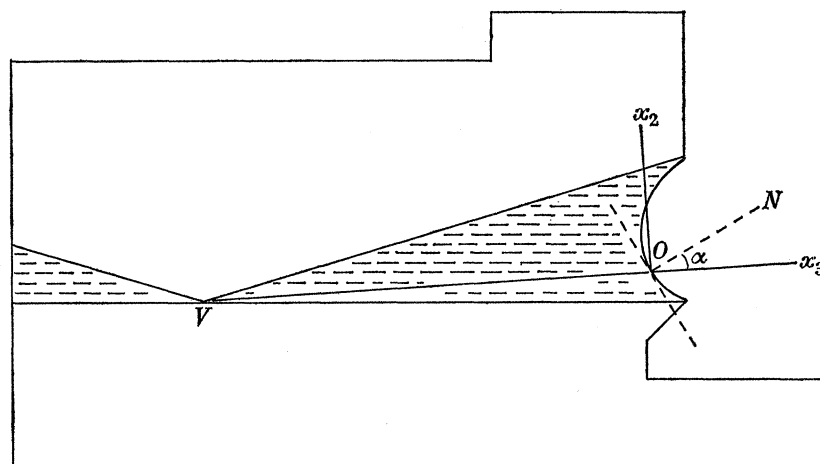


FIGURE 16. Co-ordinate system at a point O on the free liquid boundary whose normal is ON . Vertical section through cone axis.

The pressure denoted by p_R in the text represents the pressure on the plate ($-p_{22}$) (at radius R) minus the atmospheric pressure: thus $p_R = -p_{22} - p_0$, and hence (A 9) becomes

$$-p_R = p_{22} - p_{33}, \quad (\text{A } 10)$$

which is an equation used in the text.

If the free boundary is not part of a sphere of centre V , then there must be positions of O for which $\alpha \neq 0$. In this case, (A 6) can be satisfied only if $p_{21} = 0$, which is impossible; there must also be points for which $\alpha \neq \pi$ or 0 , so that $\sin 2\alpha \neq 0$ and (A 7) can be satisfied only if $p_{22} - p_{33} = 0$, which is also impossible for a general type of liquid. These inconsistencies can be resolved only by abandoning the assumption that the state of shear flow persists up to the free boundary: one can then return to the boundary conditions in the form (A 1, 4, 5) with p_{31} and p_{32} different from zero, and (A 10) must be replaced by

$$-p_R = (p_{22} - p_{33}) \cos^2 \alpha - p_{32} \sin 2\alpha. \quad (\text{A } 11)$$

In any case, the value of $p_{22} - p_{33}$ here no longer refers to a state of shear flow of the type under investigation and so (A 11) would not be of direct interest.

It follows that the use of rim pressure p_R as a means of determining $p_{22} - p_{33}$ in shear flow is not valid when the free boundary is not part of a sphere of centre V and radius R , when the effects of surface tension are negligible. While it is not clear how the effects of surface

tension should be treated in the analysis, it would appear to be unlikely that they could overcome this objection to the use of equation (A 10), but if they could they would need to be of sufficient magnitude to give terms comparable with the terms in (A 1, 4) and must therefore give important contributions to the equation which would then replace (A 10): thus (A 10) in any case is inapplicable when $\alpha \neq 0$.

(b) *Total thrust*

It is convenient to include here a derivation of the relation between total thrust in the cone-and-plate system and $p_{11} - p_{22}$, when the assumed state of shear flow persists up to the rim $r = R$. Equation (2.7) gives, on integration, the equation

$$p_{22}(r) = p_{22}(R) + (p_{11} + p_{22} - 2p_{33}) \ln(r/R), \quad (\text{A } 12)$$

since $p_{11} + p_{22} - 2p_{33}$ is here independent of r . The total downward thrust F on the plate due to the normal stress differences is given by

$$F = - \int_{r=0}^R p_{22}(r) d(\pi r^2) - p_0 \pi R^2,$$

(by subtracting the contribution from atmospheric pressure). Using the expression for $p_{22}(r)$ given in (A 12), we obtain the result

$$\begin{aligned} F &= - [p_{22}(R) + p_0] \pi R^2 + \frac{1}{2} \pi R^2 (p_{11} + p_{22} - 2p_{33}), \\ &= - [p_{33}(R) + p_0] \pi R^2 + \frac{1}{2} \pi R^2 (p_{11} - p_{22}). \end{aligned} \quad (\text{A } 13)$$

The last step involves transferring $\pi R^2 (p_{22} - p_{33})$ from the second term to the first term on the right-hand side using the fact that $p_{22} - p_{33}$ is independent of r .

If the free boundary is part of a sphere of centre V , so that the boundary condition (A 9) is valid, then this implies that the first term on the right-hand side of (A 13) is zero, and hence that

$$F = \frac{1}{2} \pi R^2 (p_{11} - p_{22}), \quad (\text{A } 14)$$

which is an equation used in the literature (Jobling & Roberts 1959). The validity of this equation is thus tied up with that of (A 9) or (A 10) and its use is therefore liable to introduce error when the free boundary is not part of a sphere of centre at the cone vertex.

(c) *Shear rate*

We now estimate the error involved in assuming that the shear rate in the cone-and-plate system is constant throughout the gap and given by equation (2.5), when the state of flow is a state of shear flow as assumed in §2(ii).

Using the spherical polar co-ordinate system of §2, and the appropriate values for g_{ij} and for the Christoffel symbols involved in the covariant derivatives in (2.2) (cf. Madelung 1943), equations (2.2) and (2.3) lead to the equation

$$G = \sin \theta (d\omega/d\theta), \quad (\text{A } 15)$$

where ω is the angular velocity of an infinitesimally thin liquid cone of semi-vertical angle θ . The stress equation of motion (Love 1944) relating to the ϕ -co-ordinate reduces to

$$\partial(p_{21} \sin \theta) / \partial \theta = 0 \quad (\text{A } 16)$$

NORMAL STRESS DIFFERENCES IN STEADY SHEAR FLOW 183

for the case of steady flow when account is taken of equation (2.1) and the fact that the physical components of stress must be independent of ϕ owing to the rotational symmetry of the system when the liquid is homogeneous.

When the variation of shear rate G across the gap is small, it is legitimate, in order to estimate the magnitude of this variation, to neglect the dependence of viscosity η on shear rate. Since $p_{21} = \eta G$, equation (A 16) then gives the result

$$G = G_0 \operatorname{cosec}^2 \theta, \quad (\text{A } 17)$$

where G_0 denotes the value of G at the plate ($\theta = \pi/2$). Thus G increases steadily as θ varies from $\pi/2$ to $\pi/2 - \theta_0$, where θ_0 is the gap angle; the total percentage variation of G across the gap calculated from (A 17) is given in table 2 for various values of the gap angle.

It is also useful to estimate the error in using the approximate formula (2.5), which in the present notation becomes

$$G_0 = \Omega/\theta_0, \quad (\text{A } 18)$$

where Ω is the angular velocity of the cone and the plate is at rest. From (A 15, 17), on eliminating G and integrating, we obtain the equation

$$\Omega = G_0 \int_0^{\theta_0} \sec^3 \beta \, d\beta \quad (\text{A } 19)$$

$$= G_0(\theta_0 + A\theta_0^3), \quad (\text{A } 20)$$

where $3 < A < 4$ when the gap angle does not exceed 10° . The last equation can be obtained from a Maclaurin expansion for the definite integral in powers of θ_0 , using Lagrange's expression for the remainder after the term in θ_0^2 . Thus the use of (A 18) corresponds to neglect of the term in θ_0^3 in (A 20); the corresponding error in G_0 calculated from (A 20) for various gap angles is given in table 2.

TABLE 2

gap angle (degrees)	variation of shear rate across gap (%)	error in using the formula $G_0 = \Omega/\theta_0$ (%)
1	0.03	0.02
2	0.21	0.08
3	0.28	0.18
4	0.49	0.32
5	0.77	0.50
7	1.5	0.98
10	3.1	2.0

The authors are greatly indebted to the Council and Directors of Research of the former British Rayon Research Association for providing the facilities necessary for the above work and for a generous gift of apparatus and money to enable the work to be continued at the Manchester College of Science and Technology. The authors would also like to acknowledge their indebtedness to Dr J. M. Garcia for data included in figures 6 and 7; to Dr J. Parker for his measurements of the 3° cone; to Messrs J. Baker and J. McConnell for their contributions to the design and construction of the apparatus; to Professor R. S. Rivlin for advice concerning the boundary conditions considered in part (a) of the

Appendix; and to Professor K. Weissenberg, Dr L. R. G. Treloar, Dr D. W. Saunders, Mr J. E. Roberts and Mr K. J. Butler, for their help and advice at many points during the course of this work.

REFERENCES

- Adams, N. 1960 *Rheol. Abstr.* **3**, no. 3, 28.
- Attree, V. H. 1952 *Electron. Engng.* **24**, 284.
- Brodnyan, J. G., Gaskins, F. H. & Philippoff, W. 1957 *Trans. Soc. Rheol.* **1**, 109.
- Coleman, B. D. & Noll, W. 1959 *Arch. Rat'l. Mech. Anal.* **3**, 289.
- Garner, F. H., Nissan, A. H. & Wood, G. F. 1950 *Phil. Trans. A*, **243**, 37.
- Greensmith, H. W. and Rivlin, R. S. 1953 *Phil. Trans. A*, **245**, 399.
- Jobling, A. & Roberts, J. E. 1959 *J. Polym. Sci.* **36**, 421.
- Kotaka, T., Kurata, M. & Tamura, M. 1959 *J. Appl. Phys.* **30**, 1705.
- Lodge, A. S. 1956 *Trans. Faraday Soc.* **52**, 120.
- Lodge, A. S. 1960a *Rheol. Abstr.* **3**, no. 3, 21.
- Lodge, A. S. 1960b *J. Sci. Instrum.* **37**, 401.
- Lodge, A. S. 1961a *Rheol. Abstr.* **4**, no. 3, 29.
- Lodge, A. S. 1961b *Polymer*, **2**, 195. (Part I).
- Love, A. E. H. 1944 *The Mathematical theory of elasticity*, 4th edn. p. 91. New York: Dover.
- Madelung, E. 1943 *Mathematische Hilfsmittel des Physikers*, p. 146. New York: Dover.
- Markovitz, H. 1957 *Trans. Soc. Rheol.* **1**, 37.
- Oldroyd, J. G. 1958 *Proc. Roy. Soc. A*, **245**, 278.
- Pollett, W. F. O. 1955 *Brit. J. Appl. Phys.* **6**, 199.
- Roberts, J. E. 1957 *Nature, Lond.* **179**, 487.
- Stefan, M. J. 1869 *Sitz. ber. Akad. Wiss. Wien. Math. Naturw. Kl. Abt. II*, **69**, 713.
- Taylor, G. I. & Saffman, P. G. 1957 *J. Aero. Sci.* **24**, 553.
- Thom, A. & Apelt, C. J. 1958 *Rep. Memor. Aero. Res. Coun.* no. 3090. London: H.M.S.O. Also private communication.
- Trapeznikov, A. A., Morozov, A. S. & Petrzhik, G. G. 1960 *Dokl. Akad. Nauk. S.S.S.R.* **133**, 637. (Cf. *Chem. Abs.* 1961, **55**, 11030d.)
- Ward, A. F. H. & Lord, P. 1957 *J. Sci. Instrum.* **34**, 263.
- Weissenberg, K. 1947 *Nature, Lond.* **159**, 310.